Chloroplast ATP synthase biogenesis requires peripheral stalk subunits AtpF and ATPG and stabilization of atpE mRNA by OPR protein MDE1

Frédéric Chaux, Domitille Jarrige, Marcio Rodrigues-azevedo, Sandrine Bujaldon, Oliver D Caspari, Shin-ichiro Ozawa, Dominique Drapier, Olivier Vallon, Yves Choquet, Catherine de Vitry

▶ **To cite this version:**

Frédéric Chaux, Domitille Jarrige, Marcio Rodrigues-azevedo, Sandrine Bujaldon, Oliver D Caspari, et al.. Chloroplast ATP synthase biogenesis requires peripheral stalk subunits AtpF and ATPG and stabilization of atpE mRNA by OPR protein MDE1. Plant Journal, 2023, 116 (6), pp.1582-1599. 10.1111/tpj.16448 . hal-04311517

HAL Id: hal-04311517
https://hal.science/hal-04311517

Submitted on 28 Nov 2023

HAL is a multi-disciplinary open access archive for the deposit and dissemination of scientific research documents, whether they are published or not. The documents may come from teaching and research institutions in France or abroad, or from public or private research centers.

L'archive ouverte pluridisciplinaire **HAL**, est destinée au dépôt et à la diffusion de documents scientifiques de niveau recherche, publiés ou non, émanant des établissements d'enseignement et de recherche français ou étrangers, des laboratoires publics ou privés.

Check for updates

the plant journal

SEB SOCIETY FOR EXPERIMENTAL BIOLOGY

The Plant Journal (2023) doi: 10.1111/tpj.16448

Chloroplast ATP synthase biogenesis requires peripheral stalk subunits AtpF and ATPG and stabilization of *atpE* mRNA by OPR protein MDE1

Frédéric Chaux[*,†], Domitille Jarrige[‡], Marcio Rodrigues-Azevedo[§], Sandrine Bujaldon, Oliver D. Caspari[¶], Shin-Ichiro Ozawa[#], Dominique Drapier, Olivier Vallon, Yves Choquet and Catherine de Vitry[*]

Unité Mixte de Recherche (UMR) 7141, Centre National de la Recherche Scientifique (CNRS) and Sorbonne Université, Institut de Biologie Physico-Chimique, 13 rue Pierre et Marie Curie, F-75005 Paris, France

Received 17 May 2023; revised 15 August 2023; accepted 21 August 2023.
*For correspondence (e-mail fchauxj@irb.hr; catherine.devitry@ibpc.fr)
[†]Present address: Ruder Boskovic Institute, Zagreb, Croatia
[‡]Present address: Génétique Moléculaire, Génomique, Microbiologie (GMGM), Université de Strasbourg, UMR 7156 CNRS, Strasbourg, France
[§]Present address: Doctoral School of Plant Sciences (SEVE) – ED567 Université Paris-Saclay,
[¶]Present address: Institut für Mikrobiologie und Biotechnologie, Rheinische Friedrich-Wilhelms-Universität Bonn, Bonn, Germany
[#]Present address: Institute of Plant Science and Resources, Okayama University, Kurashiki, Japan

SUMMARY

Chloroplast ATP synthase contains subunits of plastid and nuclear genetic origin. To investigate the coordinated biogenesis of this complex, we isolated novel ATP synthase mutants in the green alga *Chlamydomonas reinhardtii* by screening for high light sensitivity. We report here the characterization of mutants affecting the two peripheral stalk subunits *b* and *b′*, encoded respectively by the *atpF* and *ATPG* genes, and of three independent mutants which identify the nuclear factor MDE1, required to stabilize the chloroplast-encoded *atpE* mRNA. Whole-genome sequencing revealed a transposon insertion in the 3′UTR of *ATPG* while mass spectrometry shows a small accumulation of functional ATP synthase in this knock-down *ATPG* mutant. In contrast, knock-out *ATPG* mutants, obtained by CRISPR-Cas9 gene editing, fully prevent ATP synthase function and accumulation, as also observed in an *atpF* frame-shift mutant. Crossing ATP synthase mutants with the *ftsh1-1* mutant of the major thylakoid protease identifies AtpH as an FTSH substrate, and shows that FTSH significantly contributes to the concerted accumulation of ATP synthase subunits. In *mde1* mutants, the absence of *atpE* transcript fully prevents ATP synthase biogenesis and photosynthesis. Using chimeric *atpE* genes to rescue *atpE* transcript accumulation, we demonstrate that MDE1, a novel octotricopeptide repeat (OPR) protein, genetically targets the *atpE* 5′UTR. In the perspective of the primary endosymbiosis (~1.5 Gy), the recruitment of MDE1 to its *atpE* target exemplifies a nucleus/chloroplast interplay that evolved rather recently, in the ancestor of the CS clade of Chlorophyceae, ~300 My ago.

Keywords: ATP synthase, ATPG, AtpF, organellar trans-acting factor, helical repeat protein, OPR, FTSH protease, CRISPR-Cas9, *Chlamydomonas reinhardtii*.

INTRODUCTION

In almost all living cells, ATP is mainly generated by F-type ATP synthases. These 'splendid molecular machines' (Nobel Prize P. D. Boyer) are multi-subunit nanomotors made of a transmembrane moiety (F_o) comprising a rotor, which is put in motion by the dissipation of the transmembrane proton gradient, and a protruding stator part, where the phosphorylation of ADP into ATP takes place in the hydrophilic head of the soluble moiety (F_1). The crucial coupling between chemiosmotic flow and phosphorylation relies both on the central stalk spinning along with the rotor, and the peripheral stalk connecting F_1 to F_o and acting as a stator. Interestingly, the ATP synthase, as most bioenergetics complexes of eukaryotes' organelles, is a 'genetic mosaic' since some subunits are encoded in the mitochondrial or plastid genomes and others in the nuclear genome.

The subunit composition of the ATP synthase is conserved between bacteria and plastids (names of the chloroplast proteins are indicated between brackets). The rotor comprises a homo-oligomer of 8 to 14 subunits *c* (AtpH) forming a barrel-like structure. One after the other, each subunit *c* exchanges protons with the stator subunit *a* (AtpI), which provides the second half of a proton channel

© 2023 The Authors.
The Plant Journal published by Society for Experimental Biology and John Wiley & Sons Ltd.
This is an open access article under the terms of the Creative Commons Attribution License, which permits use, distribution and reproduction in any medium, provided the original work is properly cited.

spanning the membrane. The scrolling of the *c* oligomer as protons cross the membrane down their electrochemical gradient drives the rotation of the central stalk formed by the subunits γ (ATPC) and ε (AtpE). The central stalk asymmetrically protrudes in the cavity of the catalytic head, inducing conformational changes that fuel a 3-step cycle: recruitment of ADP and Pi, ATP synthesis and ATP release. The head is composed of an alternation of 3 α (AtpA) and 3 β (AtpB) subunits and is capped by subunit δ (ATPD). The catalytic head remains static relative to the rotor due to a peripheral stalk anchored in the membrane and bound to subunit *a*. The peripheral stalk is a homodimer b_2 in most bacteria and a heterodimer *bb′* (AtpF and ATPG) in cyanobacteria and thylakoids. Hence, we aimed to understand how cells reach the complicated stoichiometry of ATP synthase ($\alpha_3\beta_3\gamma\delta\varepsilon abb'c_{8\text{-}14}$ or $A_3B_3CDEIFGH_{8\text{–}14}$).

In cyanobacteria, the obtention of ATP synthase mutants is limited by its absolute requirement in both the respiratory and photosynthetic chains. In *Arabidopsis*, ATP synthase subunits required for the accumulation of chloroplast ATP synthase are also required for chloroplast development, as is the case in the seedling lethal *atpG-ko* mutant (Kong et al., 2013). The model green microalga *Chlamydomonas reinhardtii* is a facultative phototroph that can use acetate as a reduced carbon source to readily grow heterotrophically in the dark, while nonetheless retaining normal chloroplast biogenesis in the absence of photosynthesis. *C. reinhardtii* mutants have previously been isolated for each subunit of the chloroplast ATP synthase except *ATPG* (Drapier et al., 2007; Finazzi et al., 2009). This collection and few other nuclear mutants (whose causal mutations were not known at the time) have notably revealed that the control of subunit synthesis in the chloroplast is mainly post-transcriptional and that assembly intermediates control translation of the chloroplast-encoded subunits (Drapier et al., 1992, 2007; Lemaire & Wollman, 1989a, 1989b). Overall, the pleiotropic loss of all subunits in ATP synthase mutants suggests that each is required for the accumulation of the other subunits at the WT level. However, differences in stability can be observed, which allow insights into how the assembly of the ATP-synthase complex proceeds and is regulated. Peripheral membrane CF_1 subunits α, β, and γ can accumulate to some extent in the absence of CF_o transmembrane subunits, while the reverse does not occur (Lemaire & Wollman, 1989a, 1989b). This concerted accumulation occurs via the control of synthesis and/or the degradation of unassembled subunits (Choquet & Wollman, 2022; Drapier et al., 2007).

Regarding control of synthesis, the β subunit is required to activate in trans the translation of subunit α but the translation of subunit β itself is inhibited by an oligomer of α and β in the absence of γ (Drapier et al., 2007). Also, subunit β does not bind to CF_o in the absence of subunit α. Anchoring of CF_1 to the membrane requires the peripheral stalk subunit *b* and rotor subunit *c* but neither the stator subunit *a* nor the rotor subunit ε. Thus, the peripheral stalk appears to be required for anchoring CF_1 while subunit *a* is recruited later to prevent leakage of the proton gradient through assembly intermediates. The synthesis of the ε subunit even requires the accumulation of several subunits: α, β, *b*, and *c* (but not *a*) (Lemaire & Wollman, 1989a, 1989b). Thylakoid membranes of *Chlamydomonas* accumulate very little α and β subunits in an *atpE* mutant lacking ε (*Fud17*), pointing to its important role in the assembly/stabilization of ATP synthase (Lemaire & Wollman, 1989b; Robertson et al., 1990). Since peripheral stalk subunits AtpF and ATPG are ancient paralogs and very similar structurally, one may question their interchangeability. The *Fud18 Chlamydomonas* mutant lacking AtpF (Lemaire & Wollman, 1989b) does not accumulate ATP synthase, refuting that homodimeric ATPG may form an alternative peripheral stalk. To analyze the eventuality of homodimeric AtpF peripheral stalk in *Chlamydomonas*, we isolated and characterized *atpG* mutants in this work.

Chloroplast proteases rapidly degrade some subunits when they cannot assemble within a complex or when they are misfolded or damaged, for example, in photoinactivated photosystem II (Schroda & de Vitry, 2022; van Wijk, 2015). In contrast with regulations of synthesis, the role of protein degradation in the quality control of ATP synthase is poorly known. The stromal ClpP protease plays a role in the degradation of unassembled CF_1 subunits (Majeran et al., 2019), and we investigated in this work the role of FTSH, the major protease of the thylakoid, in the degradation of non-assembled ATP synthase subunits.

Nucleus-encoded factors control plastid gene expression in most cases in a gene-specific manner: M factors are involved in mRNA maturation and stabilization while T factors activate mRNA translation (Choquet & Wollman, 2002; Hammani et al., 2014). Small RNA sequencing revealed footprints at the 5′ end of most *Chlamydomonas* chloroplast mRNAs, suggesting that many M factors remain to be molecularly identified (Cavaiuolo et al., 2017). For example, the non-photosynthetic mutant strain *CAL014.01.30* (Dent et al., 2005) has been named *mde1* because RNA blots and small RNA sequencing revealed altered Maturation/stabilization of the complex D (ATP synthase) subunit AtpE mRNA, and it lacked the footprint at the 5′ end of the mature *atpE* mRNA (Cavaiuolo et al., 2017), but the mutated gene had not been identified. Recently, however, a few nucleus-encoded factors related to ATP synthase have been characterized. The MDA1 (Viola et al., 2019) and TDA1 (Eberhard et al., 2011) proteins bind to the 5′ untranslated region (UTR) of the *atpA* transcript to promote respectively its maturation/stabilization and its translation. The MTHI1 protein stabilizes the *atpH* transcript and binds to *atpH* and *atpI* 5′UTRs to promote the translation of the downstream coding sequence (CDS)

© 2023 The Authors.

1365313x, 0, Downloaded from https://onlinelibrary.wiley.com/doi/10.1111/tpj.16448 by Portail BibCNRS INSB, Wiley Online Library on [28/11/2023]. See the Terms and Conditions (https://onlinelibrary.wiley.com/terms-and-conditions) on Wiley Online Library for rules of use; OA articles are governed by the applicable Creative Commons License

(Ozawa et al., 2020). Moreover, a gain-of-function mutation in the *NCC1* gene allows it to bind to the CDS the of *atpA* transcript and to destabilize it (Boulouis et al., 2015). Interestingly, all these factors are octotricopeptide repeat (OPR) proteins. In the green lineage, large helical repeat proteins contribute to post-transcriptional regulations, such as the tetratricopeptide repeat (TPR), pentatricopeptide repeat (PPR), and OPR proteins, which comprise repeats of degenerate RNA-binding motifs of 34, 35 and 38 amino acids, respectively. In PPRs, recognition of the target transcript is driven by the binding of each motif to a preferred nucleotide, determined by the amino-acid properties at the 5th and 35th positions (Barkan et al., 2012; Yan et al., 2019). In *C. reinhardtii*, OPR proteins, with around 120 detected so far in the genome (Jarrige, 2019; *Chlamydomonas reinhardtii* CC-4532 v6.1 genome), are far more numerous than PPRs (Eberhard et al., 2011; Tourasse et al., 2013). Our current understanding is that, as for PPRs, each OPR domain interacts with one nucleotide, but the 'OPR code' is still imprecise due to the limited number of identified OPR protein/RNA target pairs.

Here, we screened transformants from random nuclear mutagenesis and presented the phenotype of several new ATP synthase mutants. By whole genome sequencing, we identify new mutants in *ATPG* and *MDE1*, the latter encoding a novel OPR protein. We also identify the previously unknown mutation of the mutant strain *CAL014.01.30* in the same gene. We provide genetic evidence that MDE1 interacts with the 5′UTR of the *atpE* transcript to stabilize it. For thorough comparison, we also genotyped the previously unidentified *atpF-Fud18* mutant (Lemaire & Wollman, 1989b). Knock-out *atpG* mutants were obtained by CRISPR-Cas9 technology and we show by mass spectrometry and protein blot analysis that knockdown of *ATPG* decreases the accumulation of the other ATP synthase subunits, while its knock-out completely prevents it. This shows that a heterodimeric AtpF-ATPG peripheral stalk is required for ATP synthase assembly. We evidence an FTSH-dependent degradation of misassembled AtpH subunit.

RESULTS

Isolation of chloroplast ATP synthase mutants by nuclear transformation

C. reinhardtii photosynthesis mutants grown in the presence of acetate as a reduced carbon source (TAP medium) can be easily screened by chlorophyll fluorescence in a non-invasive manner (Johnson et al., 2009). In an attempt to obtain mutants in the FTSH and EGY1 thylakoid proteases, we obtained four ATP synthase mutants, identified by the light sensitivity of their electron transport capacity (Majeran et al., 2001). About 2000 mutagenized clones were exposed to high light for 1 h. In colonies *F292*, *F28N*, *E236*, and *E271*, the maximal fluorescence yield of PSII, F_V/F_M, decreased drastically, as in the control *ftsh1-1* strain which cannot fulfill PSII repair (Malnoë et al., 2014; Wang et al., 2017) but not in the wild-type (WT) strain or the complemented C17 strain *ftsh1-1*::pSL18-FTSH1 (Malnoë et al., 2014; Figure 1a). We further compared the growth of our mutants on minimal (MIN) or on TAP media under increasing light intensities to that of the WT, *ftsh1-1*, and *mdb1* mutant strains, the latter lacking the nucleus-encoded M factor MDB1 required for the accumulation of *atpB* transcript (Drapier et al., 1992; Figure 1b). In TAP, mutants *E271*, *F28N*, *F292*, and *mdb1* could grow under moderate light (25 μmol photon m^{-2} sec^{-1}), although slightly less than WT, growth was almost completely suppressed by higher light (120 μmol photon m^{-2} sec^{-1}), further confirming their photosensitive phenotype. In MIN, they were not able to grow at all, suggesting that photosensitivity in *E271*, *F28N*, and *F292* mutants originates from a strong impairment of photosynthesis, as observed in the *mdb1* control. In contrast, the growth of mutant *E236* under moderate light was similar to that of WT and *ftsh1-1* in TAP and was not completely abolished in MIN; under higher light, *E236* exhibited slower growth than WT in TAP and full inhibition in MIN, similar to the *ftsh1-1* phenotype.

Sensitivity to high light can be caused by all sorts of mutations, among which deficiencies in CF_1F_o ATP synthase (Majeran et al., 2001), RuBisCO (Johnson, 2011), or FTSH (Malnoë et al., 2014). Here, defects in ATP synthase were first assessed by analysis of chlorophyll fluorescence induction kinetics. After 3 min of illumination, the steady-state fluorescence (F_S) stabilized at a low level in the wild-type (WT) strain, while in mutant strains *E236*, *E271*, *F28N*, and *F292* it increased steadily almost up to the maximal fluorescence F_M' (Figure 1c). This phenotype has been previously reported in RuBisCO or ATP synthase mutants (Bennoun et al., 1980; Bennoun & Chua, 1976; Johnson, 2011; Majeran et al., 2001). It is attributed respectively to the gradual appearance of a bottleneck in electron flow towards CO_2 fixation and to the build-up of a very high proton gradient which downregulates PSII photochemistry. Transfer of charges across the thylakoid membrane induces changes in the transmembrane electrical field which in turn affects light absorption by carotenoids. The ensuing 'electrochromic shift' (ECS) is measured as an absorption change at 520 nm. In WT cells, upon illumination, the activity of photosystems and cytochrome b_6f generates a transmembrane gradient, which is consumed by ATP synthase (Bailleul et al., 2010). In our four mutants, decay of the ECS signal was much slower than in the WT (Figure 1d): decay rates in *F28N* and *E271* were similar to that of known mutants lacking essential ATP synthase genes (*ΔatpH* and *ΔatpI*), while in *E236* and *F292* mutants, they were slightly faster but still much slower than in the WT.

© 2023 The Authors.

1365313x, 0, Downloaded from https://onlinelibrary.wiley.com/doi/10.1111/tpj.16448 by Portail BibCNRS INSB, Wiley Online Library on [28/11/2023]. See the Terms and Conditions (https://onlinelibrary.wiley.com/terms-and-conditions) on Wiley Online Library for rules of use; OA articles are governed by the applicable Creative Commons License

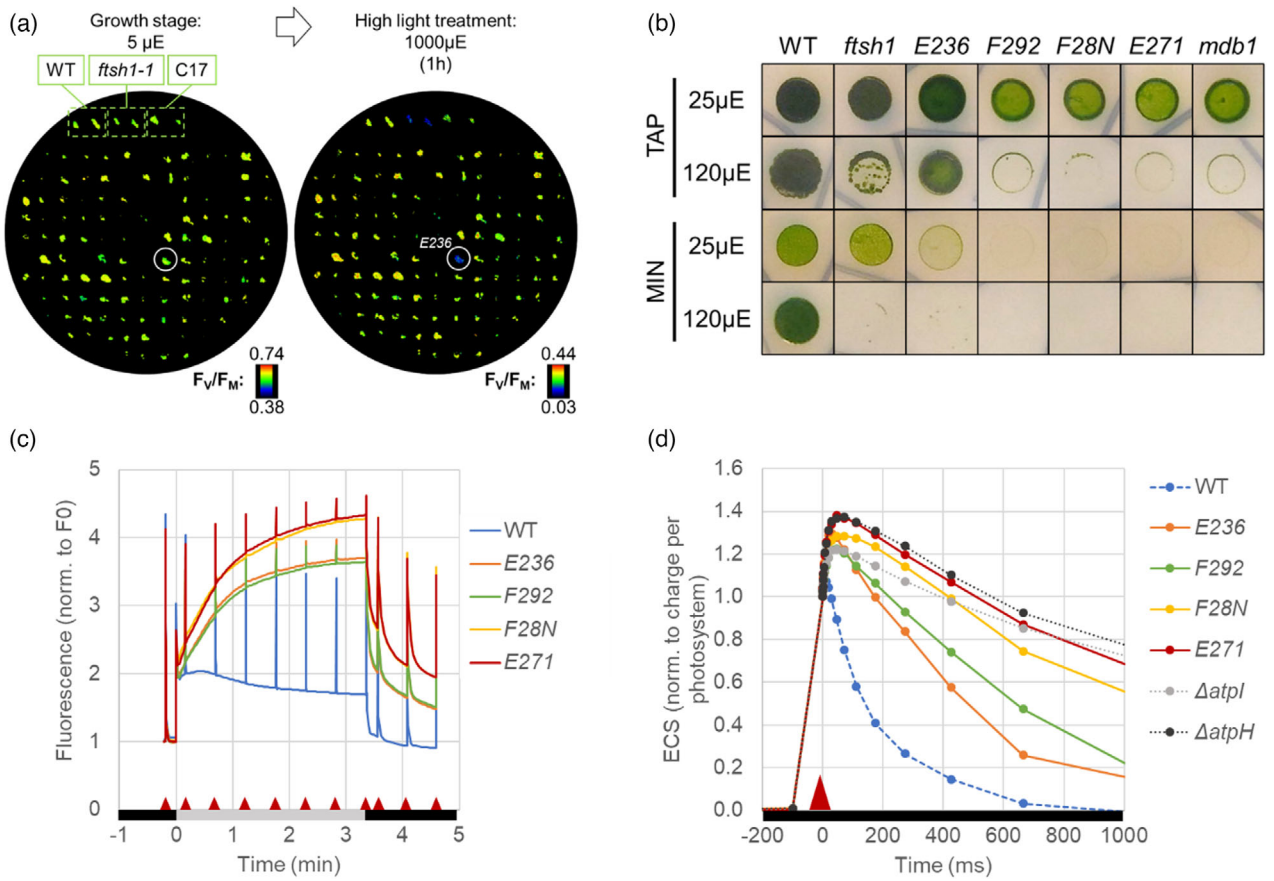

Figure 1. Isolation of chloroplast ATP synthase mutants.
(a) After mutagenesis, transformants were grown mixotrophically in low light (5 µmol photon m^{-2} sec^{-1}) for 7 days. Chlorophyll fluorescence analysis was performed before (left) and after (right) a very high light treatment (1 h, 1000 µmol photon m^{-2} sec^{-1}). Shown is the maximum quantum efficiency of PSII photochemistry F_V/F_M for the plate from which the mutant *E236* was isolated (white circle). Control strains are the wild-type (WT), *ftsh1-1* mutant and complemented *C17* strain.
(b–d) Cells were grown in dim light in TAP flasks. (b) Cells were spotted onto plates containing TAP (top panels) and minimal (MIN, bottom panels) and grown for 6 days under moderate light (25 µmol photon m^{-2} sec^{-1}) or high light (120 µmol photon m^{-2} sec^{-1}). Control strain *mdb1*, *ΔatpH* and *ΔatpI* lack ATP synthase (see main text) (c). Chlorophyll fluorescence kinetics were monitored in the transition from dark (black box) to moderate light (gray box). Red triangles indicate saturating pulses to estimate the PSII yield. (d) Kinetics of electrochromic shift of carotenoids (ECS 520 nm) upon single-turnover excitation (signal normalized to one electron photosystem^{-1}).

Accumulation of ATP synthase subunits is reduced

To gain insight into these mutant phenotypes, we investigated the accumulation of RuBisCO and individual subunits of ATP synthase by immunodetection (Figure 2). The *mrl1* strain provides a control for a non-photosynthetic strain devoid of RuBisCO but unaffected in the ATP synthase. The RuBisCO large subunit was absent in the *mrl1* mutant but accumulated to WT levels in the other mutants, showing that *E236*, *E271*, *F28N*, or *F292* strains are not RuBisCO mutants (Figure 2a). ATP synthase subunits AtpA, AtpB and AtpE (Figure 2b–d) belong to the soluble moiety (CF_1), which assembles in the stroma (Lemaire & Wollman, 1989a, 1989b), while AtpH (Figure 2d) is part of the transmembrane moiety (CF_o) (ATP synthase structure/function schematically depicted in Figure 2e,f). As controls, we used *ΔatpB*, *ΔatpH*, and *ΔatpI* deletion strains as well as the *mda1*, *mdb1*, and *mrl1* nuclear mutant strains which lack the M factors required for the accumulation of chloroplast transcripts *atpA*, *atpB*, and *rbcL*, respectively (Cavaiuolo et al., 2017; Drapier et al., 1992; Johnson et al., 2010; Viola et al., 2019). The abundance of all four tested ATP synthase subunits was much lower in the four mutants than in the WT, although showing distinct patterns of accumulation, which may reflect distinct impairments in the biogenesis of ATP synthase. Subunit AtpA was detected only in *F28N* and *F292* but not in the other mutants (Figure 2b). AtpB was absent from the *mdb1* control as expected and accumulated to about one-fifth (*E236* and *F292*) or less (*F28N* and *E271*) of the WT level in the mutants (Figure 2c). Traces of subunit AtpE were detected in *ΔatpH*, *E236*, and *F292* but not in *ΔatpB*, *F28N*, or *E271* mutants (Figure 2d). Finally, no subunit AtpH was

© 2023 The Authors.

1365313x, 0, Downloaded from https://onlinelibrary.wiley.com/doi/10.1111/tpj.16448 by Portail BibCNRS INSB, Wiley Online Library on [28/11/2023]. See the Terms and Conditions (https://onlinelibrary.wiley.com/terms-and-conditions) on Wiley Online Library for rules of use; OA articles are governed by the applicable Creative Commons License

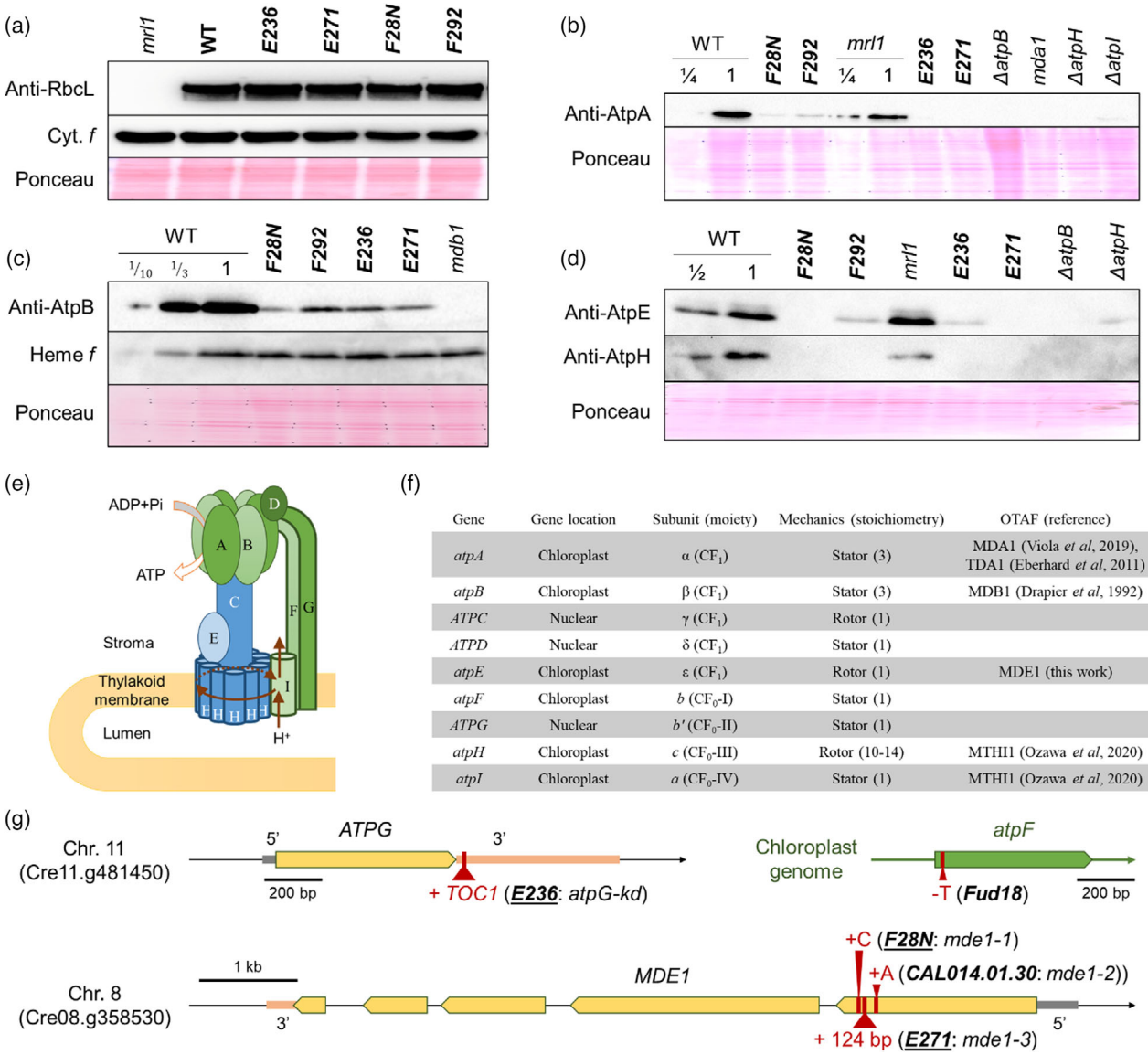

Gene	Gene location	Subunit (moiety)	Mechanics (stoichiometry)	OTAF (reference)
atpA	Chloroplast	α (CF_1)	Stator (3)	MDA1 (Viola *et al*, 2019), TDA1 (Eberhard *et al*, 2011)
atpB	Chloroplast	β (CF_1)	Stator (3)	MDB1 (Drapier *et al*, 1992)
ATPC	Nuclear	γ (CF_1)	Rotor (1)	
ATPD	Nuclear	δ (CF_1)	Stator (1)	
atpE	Chloroplast	ε (CF_1)	Rotor (1)	MDE1 (this work)
atpF	Chloroplast	*b* (CF_0-I)	Stator (1)	
ATPG	Nuclear	*b'* (CF_0-II)	Stator (1)	
atpH	Chloroplast	*c* (CF_0-III)	Rotor (10-14)	MTHI1 (Ozawa *et al*, 2020)
atpI	Chloroplast	*a* (CF_0-IV)	Stator (1)	MTHI1 (Ozawa *et al*, 2020)

Figure 2. Impairment in accumulation of chloroplast ATP synthase and candidate causal mutations.
(a–d) Whole-cell proteins were analyzed by immunoblots with the indicated antibodies (RbcL: RuBisCO large subunit; AtpA, AtpB, AtpE, AtpH: ATP synthase subunits). WT was loaded in decreasing amount as indicated by fractions. The deletion strains *ΔatpB*, *ΔatpH*, *ΔatpI* and the nuclear mutants *mda1*, *mdb1* and *mrl1* are shown as controls (detailed in main text). Ponceau red staining, heme *f* and/or Cyt. *f* provide loading controls.
(e) Simplified structure/function of chloroplast ATP synthase complex. The rotor and stator subunits are shown in blue and green, respectively. Red arrows represent the flow of protons (H^+).
(f) Genetic and structural information regarding ATP synthase subunits.
(g) Diagrams of mutations detected in the mutants (bold) at the indicated loci. Nuclear genes *ATPG* (top left) and *MDE1* (bottom) in yellow arrows (exons), 5′UTR in gray and 3′UTR in orange. Chloroplast-encoded gene *atpF* in green (CDS). + and − stand for insertions and deletion, respectively, as compared to WT. Mutants obtained in this work are underlined.

detected in any of the ATP synthase mutants, in line with previous reports that AtpH is only stable when ATP synthase is fully assembled (Ketchner et al., 1995; Lemaire et al., 1988; Lemaire & Wollman, 1989a, 1989b).

Causative mutations in *ATPG*, *atpF*, and *MDE1* genes

Altogether, this preliminary characterization indicated that the four mutants *E236*, *E271*, *F28N*, and *F292* are deficient in the chloroplast ATP synthase, with *E236* being slightly leaky. Although obtained in a transformation involving the *aphVII* cassette, the mutant phenotypes did not co-segregate with hygromycin resistance in the progeny of backcross to a WT strain revealing that the ATP synthase defect in the four mutants was genetically independent from the transgene insertion and rather due to other mutations. To identify these mutations, we sequenced the

© 2023 The Authors.

1365313x, 0, Downloaded from https://onlinelibrary.wiley.com/doi/10.1111/tpj.16448 by Portail BibCNRS INSB, Wiley Online Library on [28/11/2023]. See the Terms and Conditions (https://onlinelibrary.wiley.com/terms-and-conditions) on Wiley Online Library for rules of use; OA articles are governed by the applicable Creative Commons License

whole genome of the mutant strains *E236*, *F28N*, *F292*, and *E271* as well as the WT and *CAL014.01.30* strains by paired-end Illumina sequencing (Table S1, Figures S1 and S2) and took advantage of recent genome improvements (Craig et al., 2021; O'Donnell et al., 2020). We first looked for candidate mutations in genes known to be related to ATP synthase, namely nucleus-encoded subunits, assembly factors, and organellar trans-acting factors (OTAFs) (Rühle & Leister, 2015).

The mutant *E236* was found to carry a TOC1 transposon insertion in the 3′UTR of the *ATPG* gene (locus Cre11.g481450), about 30 bp downstream of the stop codon (Figure 2g, top left panel; Figure S1a). Mate reads mapped to distant genome locations, in all cases corresponding to one of the many copies of the *TOC1* transposon (Day & Rochaix, 1991; Kim et al., 2006). This large rearrangement prevented PCR amplification of the locus (Figure S1b). We also sequenced the chloroplast *atpF* gene in the *Fud18* mutant which specifically lacks synthesis of AtpF, the other peripheral stalk subunit (Lemaire & Wollman, 1989b). We found a thymine deletion shortly after the start codon, causing a frameshift and an early stop codon (Figure 2g, top right panel; Figure S1c).

We found three distinct mutations in the 1st exon of the same gene on chromosome 8, Cre08.g358530 (version v5; modified gene model in v6: Cr_08_37856.1) in three independent mutants (Figure 2g, bottom panel). The *F28N* and *E271* mutants carry respectively a single nucleotide insertion and an insertion of 124 bp (Figure S2a). To identify the mutation in the mutant *CAL014.01.30*, we outcrossed it to the highly polymorphic wild-type strain S1D2 and pooled the progeny into either ATP synthase-deficient or wild-type phenotypes. Sequencing both pools separately revealed that the *mde1* phenotype was linked to chromosome 8 left arm (Figure S2b). More specifically, whereas the wild-type pool showed only S1D2-inherited polymorphisms in this region, we found in the ATP synthase-deficient pool a single-nucleotide insertion in the 1st exon of gene Cre08.g358530 (Figure S2c), which likely caused the *mde1* phenotype. The insertions in mutants *F28N* and *CAL014.01.30* produce frame shifts, while the insertion in the *E271* mutant introduces a stop codon, all leading to truncated polypeptides for Cre08.g358530 (Figure S2d–f). The Cre08.g358530 locus, made of 5 exons, extends over 8.2 kb and encodes a large protein of 2175 residues that contains 12 OPR repeats. Because of its length, we failed to amplify the full gene to complement these mutants for formal identification of Cre08.g358530 as *MDE1*. However, three independent strains mutated in Cre08.g358530 lack the *atpE* transcript (see below), thus *F28N*, *CAL014.01.30*, and *E271* are likely allelic mutants of the *MDE1* gene and were therefore called *mde1-1*, *mde1-2*, and *mde1-3*, respectively.

We found in mutant *F292* no mutation in known ATP synthase-related genes nor in the photosynthesis 'Green-cut' gene set (Merchant et al., 2007). Using the impact predictor of point mutations SnpEff (Cingolani et al., 2012) and the current genome annotation, we found no difference in *F292* as compared to the WT. However, numerous *F292* reads were anchored in transposable elements (Craig et al., 2021) absent in the WT: the promoter HSP70A from our transgene integrated into *Gypsy-7* and the retrotransposon *TOC1* was found in three novel loci, which together with its transposition in the 3′UTR of *ATPG* in *E236*, suggests that *TOC1* transposition is promoted during the transformation process, possibly due to stress conditions and/or DNA damage.

In conclusion, we characterize one mutation in the CDS of the chloroplast gene *atpF* and another in the 3′UTR of the nuclear gene *ATPG*, each encoding one of the two peripheral stalk subunits of chloroplast ATP synthase (respectively subunits *b* and *b′*) whose role in assembly is investigated in the next sections. Three other mutants were found to carry frame-shift mutations in Cre08.g358530, that is, *MDE1*.

Complementation of mutant *E236* by the *ATPG* gene

To formally demonstrate that photosynthesis impairment in *E236* stems from alteration of *ATPG*, we re-introduced the WT version of *ATPG* by complementation, using the WT PCR product shown in Figure S1a (hereafter denoted $ATPG^{WT}$) and selection on minimal medium under high light. Complemented lines *E236::*$ATPG^{WT}$ C1 and C3 grew as well as the WT strain in the absence of acetate (MIN) and under high light (Figure 3a, left panel) and restored most of the PSII yield (Figure 3a, right panels, Figure 3b). The decay rate of the proton gradient (Figure 3c) and accumulation of subunits AtpB, AtpH, and ATPG in thylakoid membranes (Figure 3d) was restored to WT levels in the *C1* complemented strain *E236::*$ATPG^{WT}$. As controls, we used CF_o mutants *ΔatpH* and *atpF-Fud18*. This confirms that ATP synthase impairment in *E236* originates from the mutation in *ATPG*, providing the first mutant of subunit *b′* and the last missing mutant affecting ATP synthase subunits in *C. reinhardtii* (Finazzi et al., 2009). However, the less severe growth phenotype of *E236* compared to other ATP synthase mutants (Figures 1b and 3a) suggests that the *TOC1* insertion in the 3′UTR of *ATPG* does not fully prevent its expression. Thus mutant *E236* may be a knock-down, rather than a knock-out, of *ATPG*.

To probe the possible accumulation of reduced levels of assembled ATP synthase in *atpG-kd* (*E236*), we used mass-spectrometry to quantify the protein content in cells grown in phototrophic conditions under low light (Figure 4a). Using Benjamini-Hochberg's adjustment ($\alpha = 0.05$), accumulation levels were significantly altered in *atpG-kd* as compared to WT for 452 (15%) of the total 3105 detected proteins, among which only 3 and 18 proteins were at least twice more or twice less present in *atpG-kd* than in WT. We did not distinguish specific pathways or

© 2023 The Authors.

1365313x, 0, Downloaded from https://onlinelibrary.wiley.com/doi/10.1111/tpj.16448 by Portail BibCNRS INSB, Wiley Online Library on [28/11/2023]. See the Terms and Conditions (https://onlinelibrary.wiley.com/terms-and-conditions) on Wiley Online Library for rules of use; OA articles are governed by the applicable Creative Commons License

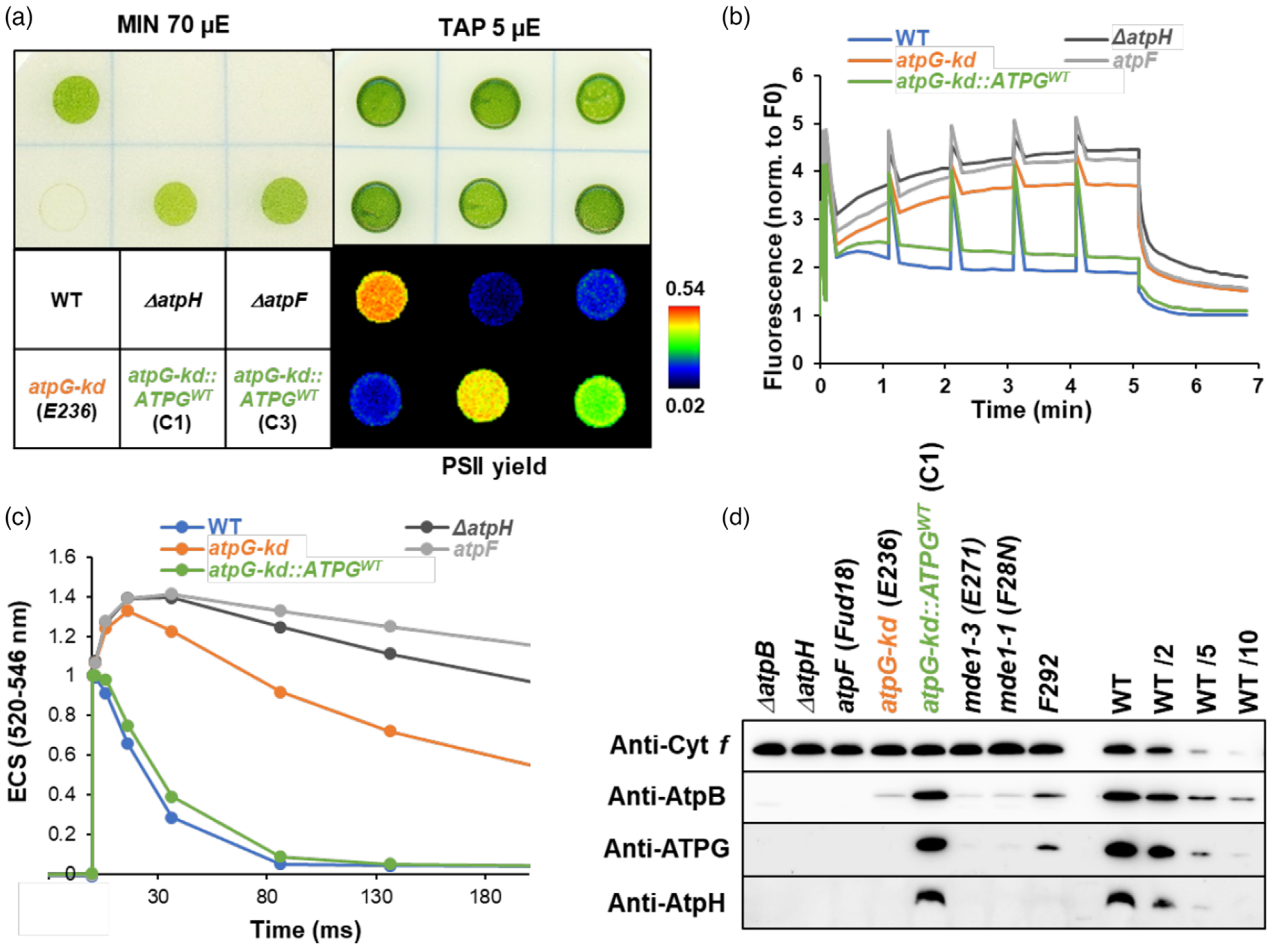

Figure 3. Photosynthesis is restored by complementing the mutant *E236* with the WT version of *ATPG*.
(a) Cells were grown phototrophically on MIN medium under moderate light (70 µmol photon m^{-2} sec^{-1}) or mixotrophically on TAP medium in low light (5 µmol photon m^{-2} sec^{-1}). PSII yield $(F_M'-F_S)/F_M'$ was assessed by chlorophyll fluorescence and shown in false-color scale.
(b) Kinetics of chlorophyll fluorescence were monitored under moderate light. Saturating light pulses were applied every minute to reach F_M' and calculate PSII yield.
(c) Kinetics of electrochromic shift (ECS) of carotenoids (520 nm) upon single-turnover excitation (signal normalized to photosystem charge separation).
(d) Thylakoid membranes were purified and content in cytochrome *f* (loading control) and ATP synthase subunits AtpB, ATPG and AtpH analyzed by immunoblot. Samples were loaded on equal chlorophyll basis (10 µg) together with a dilution series for the WT. The complemented strain C1 shown in (a) is used in (b, c and d).

functional groups of proteins that were up- or downregulated, except for the ATP synthase itself. Seven of its subunits were more than six-fold depleted in *atpG-kd* than in the WT, that are, AtpA, AtpB, ATPC, ATPD, AtpE, AtpF, and notably ATPG. The two peripheral stalk subunits, ATPG and AtpF, were most depleted, down to ~5% of WT levels. Regarding the last two ATP synthase subunits, (i) AtpH was not detected from either WT or *atpG-kd* and (ii) Atpl was detected in only five of the six replicates from WT but not detected in any sample from *atpG-kd* (Figure S3). Thus, this mutant can accumulate low levels of functional ATP synthase, allowing the dissipation of part of the proton gradient (Figure 3c) to produce ATP. This supports the weak phototrophic growth and offers a better tolerance to high light than in ATP synthase null mutants (Figures 1 and 3). In conclusion, we provide evidence that *TOC1* insertion in the 3′UTR of *ATPG* gene in mutant *E236* decreases the expression level and accumulation of ATPG protein but does not abolish it, allowing the assembly of few, functional ATP synthase complexes.

Concerted accumulation of ATP synthase subunits involves proteolysis by FTSH

Since the accumulation of ATP synthase in *atpG-kd* (*E236*) is limited by the amount of ATPG subunit, we wondered whether the other subunits possibly produced in excess were subsequently removed by proteolysis. One candidate for such proteolytic disposal is the thylakoid FTSH protease, a transmembrane FTSH1-FTSH2 hetero-hexamer, which degrades damaged subunit D1 during PSII repair cycle, cytochrome b_6f subunits and thylakoid membrane proteins involved in cytochrome b_6f biogenesis upon

© 2023 The Authors.

1365313x, 0, Downloaded from https://onlinelibrary.wiley.com/doi/10.1111/tpj.16448 by Portail BibCNRS INSB, Wiley Online Library on [28/11/2023]. See the Terms and Conditions (https://onlinelibrary.wiley.com/terms-and-conditions) on Wiley Online Library for rules of use; OA articles are governed by the applicable Creative Commons License

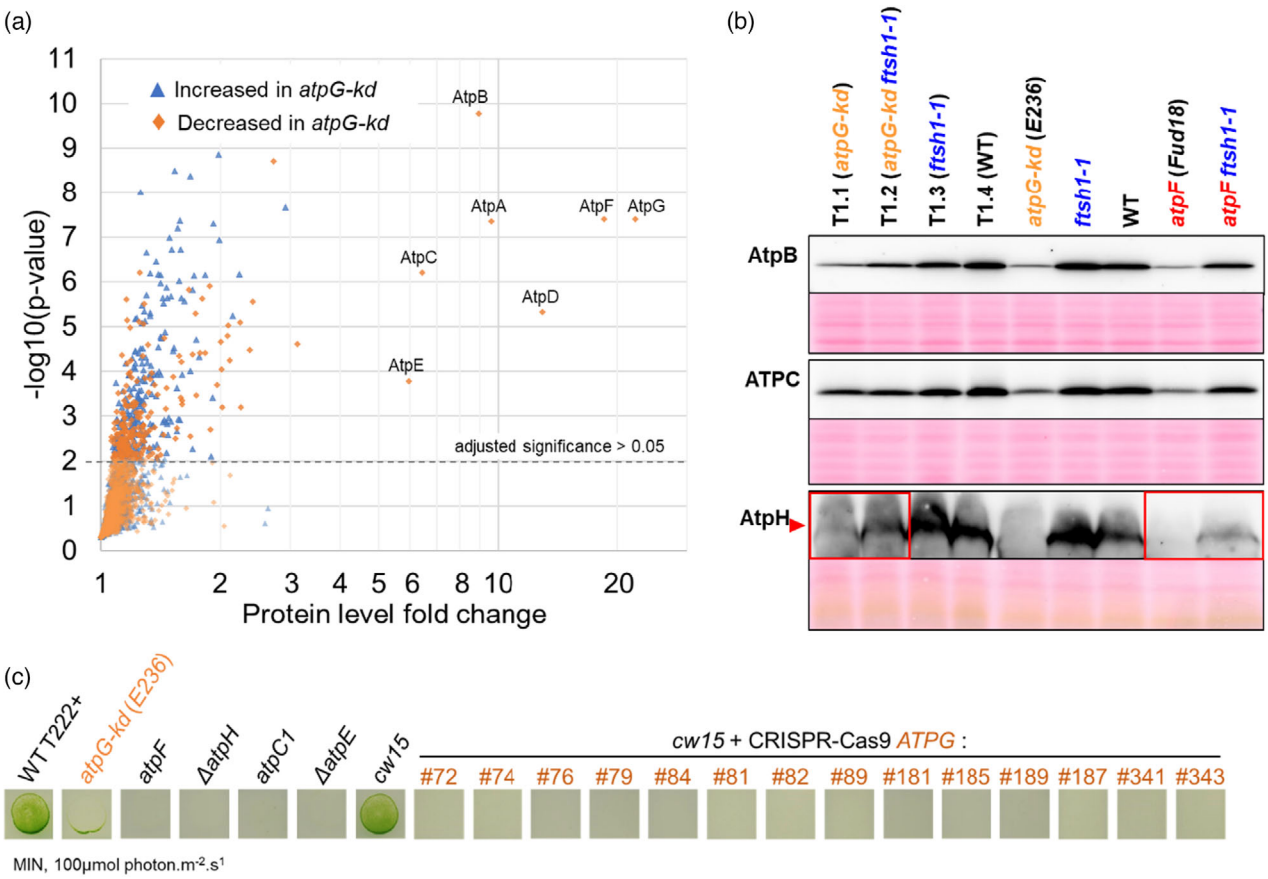

Figure 4. ATP synthase accumulation is downregulated in *E236* (*atpG-kd*), controlled by thylakoid protease FTSH, but phototrophy is abolished in CRISPR-Cas9 *atpG* mutants.

(a) WT and mutant *E236* were grown in MIN under low light. Whole cell proteins were detected by mass spectrometry and averaged over 6 replicates to determine increased (blue triangles) or decreased (orange diamonds) levels in *E236* as compared to WT (fold-change shown in log scale). Significance was assessed by unilateral *t*-tests (*P*-value shown at log scale) and adjusted according to the Benjamini-Hochberg approach. Distribution of proteins detected in less than two samples in one of the strains (no statistics available) are shown in Figure S3.

(b) The mutant *ftsh1-1* was crossed either to mutant *atpG-kd* (*E236*) or to mutant *atpF* (*Fud18*) and tetrads were dissected. Progeny and parental strains were grown in TAP under dim light and cell extracts were analyzed by western blot. Staining in Ponceau red as loading control. Red arrow points to the increased AtpH accumulation in double mutants combining ATP synthase and *ftsh1-1* mutations as compared to single ATP synthase mutants.

(c) ATPG was interrupted by CRISPR-Cas9 (Figures S5–S7). Cells of representative colonies were grown in TAP under dim light, spotted on minimal medium (MIN) and grown for 10 days under 100 µmol photon m^{-2} sec^{-1}.

nutrient starvation or in cytochrome b_6f mutants, and LHCI antenna proteins in chlorophyll *b*-less mutants (Bujaldon et al., 2017; Calderon et al., 2023; De Mia et al., 2019; Kato et al., 2023; Malnoë et al., 2011, 2014; Schroda & de Vitry, 2022; Wei et al., 2014). We thus crossed the *atpG* and *atpF* mutants to the proteolytic-defective *ftsh1-1* mutant (Malnoë et al., 2014). Subunits AtpB, ATPC, and AtpH accumulated in higher amounts in the double mutants *atpG-kd ftsh1-1* and *atpF ftsh1-1* as compared to single mutants *atpG-kd* and *atpF* (Figure 4b). We also crossed the *ftsh1-1* mutant to two CF_1 mutants (Figure S4). The *atpC1* mutant, lacking subunit γ, was crossed to an *ftsh1-1* strain carrying the H202Q mutation in the chloroplast *petB* gene (*petB** in the following). petB* here serves as a control, because we previously observed that the impaired accumulation of the cytochrome b_6f complex in this mutant was partially restored by the *ftsh1-1* allele (Malnoë et al., 2011). Indeed, the triple mutant progeny showed restored accumulation not only of the transmembrane subunit IV of cytochrome b_6f but also of AtpH (Figure S4a). In contrast, the levels of soluble subunits AtpA and AtpB were not affected by the *ftsh1* mutation. Similarly, in a cross between *ΔatpA* and *ftsh1-1*, the double mutant accumulated similar levels of AtpB and ATPC subunits but significantly more AtpH than the *ΔatpA* mutant (Figure S4b). Prior studies (Drapier et al., 2007), have shown that the absence of ATPC limits the translation of AtpB while unassembled AtpB stimulates the synthesis of AtpA. In contrast, no assembly-mediated translational regulation has been shown for AtpH (Ozawa et al., 2020), and our results suggest that AtpH level in ATP synthase mutants is largely controlled by its stability, with the FTSH protease responsible for most of its removal.

© 2023 The Authors.

1365313x, 0, Downloaded from https://onlinelibrary.wiley.com/doi/10.1111/tpj.16448 by Portail BibCNRS INSB, Wiley Online Library on [28/11/2023]. See the Terms and Conditions (https://onlinelibrary.wiley.com/terms-and-conditions) on Wiley Online Library for rules of use; OA articles are governed by the applicable Creative Commons License

ATPG is strictly required for ATP synthase biogenesis

To completely disrupt ATPG accumulation, we developed a custom CRISPR-Cas9 protocol (see Materials and Methods and Figures S5–S7), aimed at generating a targeted knock-out of *ATPG* by inserting a hygromycin resistance cassette, equipped with homology flanks, at the CRISPR-Cas9 cut site within the CDS (Figure S5a). Transformants, screened by chlorophyll fluorescence recorded directly on selection plates under medium light, revealed a large decrease in PSII yield after 3-min illumination (as in Figure 1c) in ~5% of the clones in two replicate CRISPR-Cas9 transformations (Figure S5b, left panel). To analyze the obtained mutations, the regions flanking the CRISPR-Cas9 cut site in *ATPG* were amplified by PCR using several pairs of primers in 31 putative *atpG* clones and sequenced (Figures S5–S7). Altogether, the presence of homology flanks in the co-transformation cassette ('Hygro_HR', 21 clones analyzed) allowed repair of the Cas9 cut by recombination at 23 of the 42 borders and notably yielded 8 expected mutants, proving its relative accuracy for knock-in (~38% of selected clones). In the absence of homology flanks, the co-transformation cassette ('Hygro') was inserted in *ATPG* in 4 out of 10 analyzed mutant clones. Small indels were also found in the CRISPR site ('Hygro': 3 mutants out of 10 analyzed, 'Hygro_HR': 2 out of 21), suggesting that the absence of homology flanks may be suitable to generate point mutations by imperfect non-homologous end joining (NHEJ).

The obtained *atpG* mutants were unable to grow on minimal media (Figure 4c), as other ATP synthase knock-out mutants (e.g., *ΔatpH*), while *atpG-kd* could grow slightly. In immunoblot analyses of cells of these *atpG-ko* mutants (Figure S5h), no ATPG was detected and the level of AtpB normalized to the loading control cytochrome *f* was decreased to 12 ± 3% of the wild-type level in cells of *cw15* strain. Moreover, the decay of the proton gradient measured by ECS was much longer in the *atpG* mutants tested (Figure S5i) than in the WT, as in other ATP synthase knock-out mutants but notably longer than in the *atpG-kd* (*E236*) (see Figure 1d). Thus, ATPG, just like the other peripheral stalk subunit AtpF (Lemaire & Wollman, 1989b), is absolutely required for the assembly, and thus for phototrophic growth.

MDE1 is required for the accumulation of *atpE* mRNA

The accumulation of *atpA*, *atpB*, *atpH*, and *atpI* transcripts in the mutants *E236*, *E271*, *F28N*, and *F292* were similar to that in the WT (Figure S8) as was the accumulation of *atpE* transcript in the *Fud17* mutant strain that carries a single base deletion in the *atpE* CDS (Robertson et al., 1990; Figure 5a). The *atpE* transcript, however, was absent in *F28N*, *CAL014.01.30*, and *E271*, the three strains mutated in Cre08.g358530. To identify the region of *atpE* responsible for this phenotype, we resorted to chimeric gene '*aAdE*' (Figure 5b) where the *atpE* CDS was fused in frame to the promoter and 5′UTR of the photosystem I gene *psaA*. When transformed into *mde1-1* and WT strains as a control, the *aAdE* chimera replaced the endogenous *atpE* gene and allowed the accumulation of an *atpE* transcript (Figure 5a), at a lower size because the 5′UTR of *psaA* is shorter than that of *atpE*. This construct sustained phototrophic growth and linear electron flow in both the WT and the *mde1* mutant, showing that the *psaA* 5′UTR can efficiently sustain the expression of the *atpE* CDS (Figure 5, transformants C1 and C2 in *mde1-1* background; Figure S9, transformants X1-X4 in *mde1-2* background and transformants #1–#4 in *mde1-3* background). Thus, ATP synthase can be restored in the absence of MDE1 when the 5′UTR of *atpE* is substituted by another 5′UTR (here the *psaA* 5′UTR) able to stabilize and drive the translation of the transcript.

The WT displays a footprint at the 5′ end of the *atpE* mRNA which disappears in the *mde1-2* mutant (Cavaiuolo et al., 2017), suggesting that binding of MDE1 at this site prevents degradation of the transcript by 5′–3′ exonucleases, as already shown for many chloroplast transcripts (Drager et al., 1998; Loiselay et al., 2008; Ozawa et al., 2020; Pfalz et al., 2009; Vaistij et al., 2000; Wang et al., 2015). To explore to which extent the recruitment of MDE1 on the *atpE* 5′UTR may be conserved, we analyzed the region upstream of *atpE* in representative green algae (Figure 6a,b). The *atpE* gene is ancestrally encoded downstream of *atpB* in the green lineage, notably in algae (e.g., *Ulva mutabilis* and *Tetraselmis* sp. *CCMP 881*), but is located downstream of *rps7* in most members of the class Chlorophyceae, including *Chlamydomonas* (Figure 6a, left panel). However, using the motif discovery tool MEME, we found that similarity in the *atpE* 5′UTRs is mostly limited to few regions in *C. reinhardtii*, *C. incerta*, and *C. schloesseri* on the one hand (blue boxes), or between *Volvox carteri*, *Gonium pectorale* and *Yamagishella unicoca* on the other hand (orange box). Interestingly, the MDE1 footprint found in *C. reinhardtii* (Cavaiuolo et al., 2017) corresponded to the most significant motif (yellow box in Figure 6a,b) detected in almost all Chlorophycae of the orders Chlamydomonadales and Sphaeropleales (the 'CS clade'). This suggests that this sequence emerged as the 5′ end of the mature mRNA in the ancestor of the CS clade (see Tables S5 and S6). In contrast, MDE1 orthologs were found only in genomes of the *Reinhardtinia* clade and in a few closely related species (Figure 6a; *G. pectorale* was uncertain because of a local gap in the genome assembly). We compared all candidate MDE1 orthologs and detected conserved regions (Figure 6c; Figure S10) using MEME (ungapped), GLAM2 (gap allowed), and MAST. At least 12 OPR domains were clearly identified (shown as barrel pairs). Altogether, our analyses suggest that the nuclear

© 2023 The Authors.

1365313x, 0, Downloaded from https://onlinelibrary.wiley.com/doi/10.1111/tpj.16448 by Portail BibCNRS INSB, Wiley Online Library on [28/11/2023]. See the Terms and Conditions (https://onlinelibrary.wiley.com/terms-and-conditions) on Wiley Online Library for rules of use; OA articles are governed by the applicable Creative Commons License

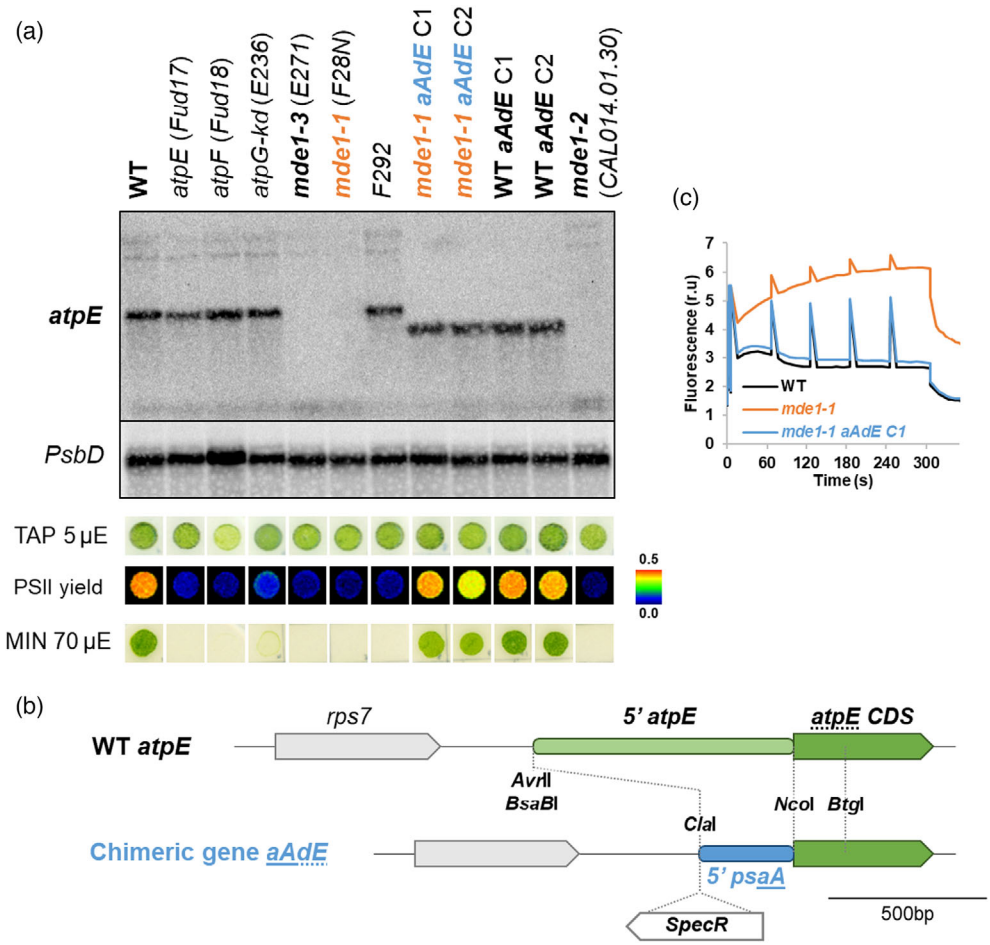

Figure 5. In absence of MDE1, accumulation of *atpE* transcript is restored by replacing its 5′UTR.
To restore *atpE* mRNA accumulation, the native *atpE* gene was replaced in *mde1-1* mutant (*F28N*) and WT (control) by a chimeric transgene 5′psaA-atpE, associated with a spectinomycin resistance gene for the selection of transformed cells. Two independent transformants are shown for each genetic context (see Figure S9 for *mde1-2* and *mde1-3*).
(a) WT and ATP synthase mutant strains were grown in dim light and accumulation of transcripts *atpE* and *PsbD* (loading control) was analyzed by RNA blot. Cells were further grown in heterotrophy (TAP, 5 µmol photon m^{-2} sec^{-1}) or in phototrophy (MIN, 70 µmol photon m^{-2} sec^{-1}). On TAP plates, PSII yield under moderate light is shown in false-color scale.
(b) Schematic representation of the *aAdE* chimera, where the *atpE* 5′-UTR has been replaced by the *psaA* 5′-UTR. Positions of the resistance cassette (Spec^r), inserted in the *atpE* orientation, and of relevant cloning sites are shown.
(c) Induction kinetics of chlorophyll fluorescence in relative units (r.u.) under moderate light. Saturating light pulses were applied every minute to reach F_M'.

factor MDE1 and its specific ~20 bp target sequence upstream of *atpE* were recruited to stabilize *atpE* mRNA in the last common ancestor of Chlamydomonadales, estimated ~500 My ago (Del Cortona et al., 2020).

DISCUSSION AND PERSPECTIVES

Chlamydomonas CF_1F_0 requirement for peripheral stalk subunits AtpF and ATPG

In the ATP synthase, AtpF and ATPG both form long helices that protrude from the membrane into the stroma and form the peripheral stalk of plastid ATP synthase, derived from the bacterial b_2 homodimer. Both peripheral stalk subunits are encoded in the chloroplast in red algae (Douglas & Penny, 1999) and red algal plastid endosymbionts (Oudot-le Secq et al., 2007), in contrast to the green algae (Gallaher et al., 2018) and land plants (Malik Ghulam et al., 2012) in which AtpF is encoded in the chloroplast and ATPG in the nucleus. Mutants of all ATP synthase subunits except ATPG had previously been isolated in *Chlamydomonas* (Drapier et al., 2007; Finazzi et al., 2009). Here, we first identified an *ATPG* knock-down mutant (*E236*) with a *TOC1* transposon insertion in the 3′UTR. To obtain a mutant in the CDS of *ATPG*, we used the CRISPR-Cas9 technology for targeted gene modification. We show that as the historical *atpF-ko* mutant, *atpG-ko* cannot accumulate CF_1F_o ATP synthase. This requirement of both ATPG and AtpF subunits indicates that neither ATPG nor AtpF homodimers can substitute for the ATPG/AtpF heterodimer peripheral stalk of *Chlamydomonas* chloroplast ATP synthase. These

© 2023 The Authors.

1365313x, 0, Downloaded from https://onlinelibrary.wiley.com/doi/10.1111/tpj.16448 by Portail BibCNRS INSB, Wiley Online Library on [28/11/2023]. See the Terms and Conditions (https://onlinelibrary.wiley.com/terms-and-conditions) on Wiley Online Library for rules of use; OA articles are governed by the applicable Creative Commons License

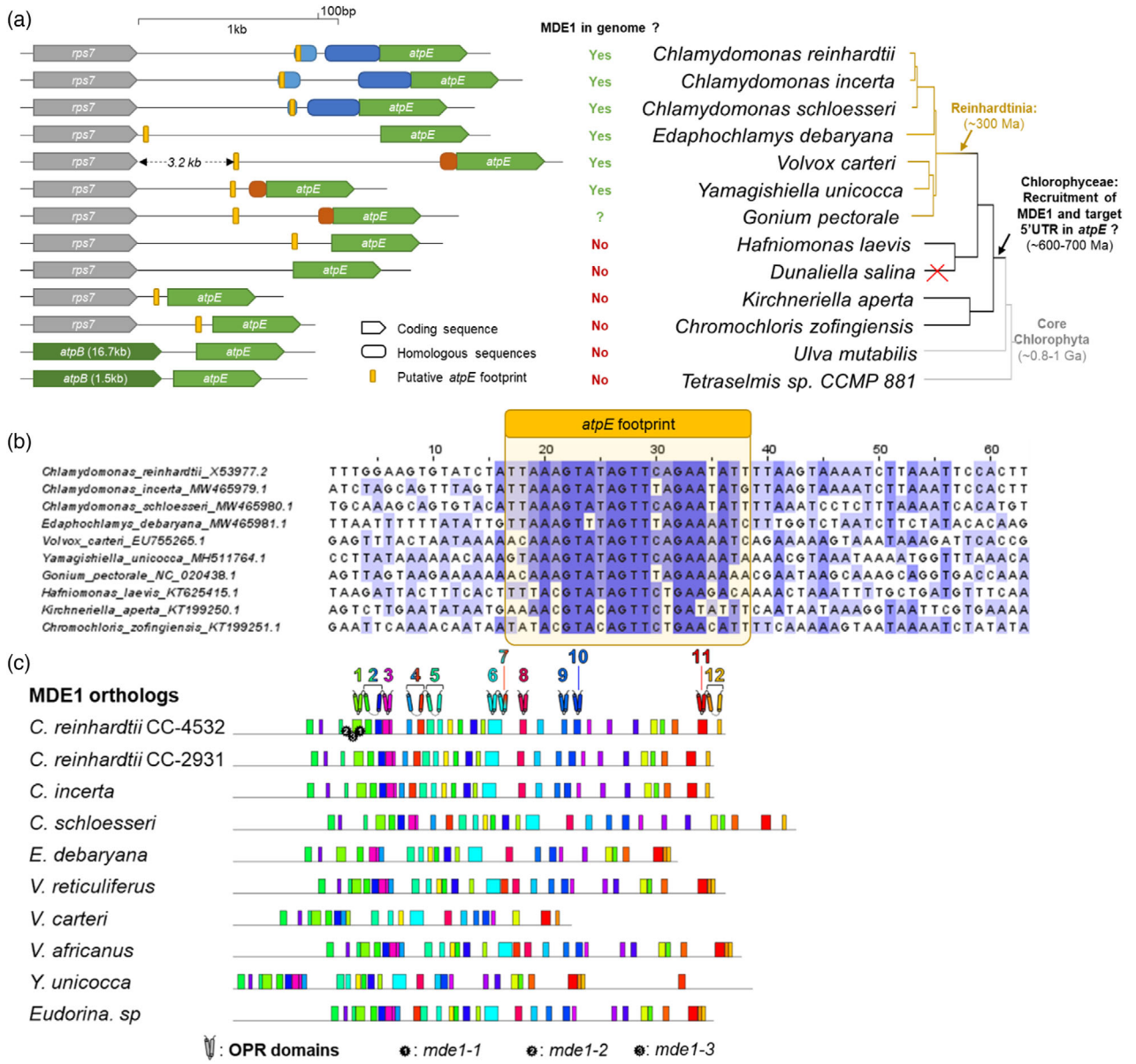

Figure 6. Conservation of *atpE* gene promoter and MDE1 protein in Volvocales and relatives.
(a) The regions upstream of *atpE* were collected from chloroplast assemblies (see accession numbers in Table S6) and compared using BLAST. Coding sequences are shown as arrows, homologous sequences are denoted as colored boxes and possible footprints shown in yellow. Sequences are represented at scale, except intergenic region in Volvox and *atpB* gene in Ulva and Tetraselmis. A species-level phylogenetic tree is displayed on the left, with branch length accounting for substition frenquency among Reinhardtinia (Craig et al., 2021); longer divergence time are shown as cladogram.
(b) Alignment of the *atpE* RNA footprint from *C. reinhardtii* and putative homologous sequences found upstream of *atpE* in Volvocales. Conserved nucleotides highlighted in blue.
(c) Domain conservation among MDE1 orthologs was assessed using MEME (30 most probable domains, encompassing 6–100 residues, present in at least 5 species; GLAM2 was used to evidence alignment gaps in domains that are thus split by MEME). OPR domains are shown as double barrels colored according to the domain boxes. Mutated sites in *mde1-1* and *mde1-2* mutant strains (*C. reinhardtii*) shown as black stars. Multiple sequence alignment and accession numbers shown in Figure S10 and Table S2, respectively. Eudorina is a genus closely related to Volvox.

mutants may further be useful for structural investigation of the peripheral stalk. Indeed, the peripheral stalk may not only be involved in preventing the CF_o-driven rotation of CF_1 but may also be animated by elastic conformational changes crucial for the energetic requirements of the ATP synthesis cycle (Hahn et al., 2018). Our work opens the door for testing spring properties either by complementation assay with mutated *AtpF* and/or *ATPG*, or *de novo* generation of CRISPR-Cas9 mutants following our approach.

© 2023 The Authors.

1365313x, 0, Downloaded from https://onlinelibrary.wiley.com/doi/10.1111/tpj.16448 by Portail BibCNRS INSB, Wiley Online Library on [28/11/2023]. See the Terms and Conditions (https://onlinelibrary.wiley.com/terms-and-conditions) on Wiley Online Library for rules of use; OA articles are governed by the applicable Creative Commons License

Transmembrane subunits of ATP synthase as substrates of the thylakoid FTSH protease

The FTSH proteases are embedded in membranes and are important in the removal of damaged, misfolded, or misassembled membrane proteins. By considering the fate of unassembled ATP synthase subunits in *ftsh* mutants, several non-assembled F_o subunits were previously shown to be substrates of FTSH proteases in bacteria and mitochondria. The bacterial ATP synthase subunit *a* is a substrate of the homo-oligomer FTSH in *Escherichia coli* (Akiyama et al., 1996). In the mitochondria of *Saccharomyces cerevisiae*, the ATP synthase F_o subunits Atp6, Atp8, and Atp9 are substrates of the hetero-oligomer FTSH protease *m*-AAA facing the matrix (Guélin et al., 1996; Pajic et al., 1994). We show in all the *Chlamydomonas* ATP synthase mutant tested (*atpG-kd*, *atpF-Fud18*, and *atpC-1* and *ΔatpA*) partial recovery of CF_o subunit AtpH accumulation occurred when the thylakoid FTSH protease was inactivated by the *ftsh1-1* mutation. This indicates that thylakoid AtpH is also a substrate of FTSH.

Interplay between MDE1 factor and *atpE* mRNA

Since the establishment of the plastid endosymbiosis in photosynthetic eukaryotes, the coupling between gene expression in the organelles and the nucleus was a major driver of evolution. In *C. reinhardtii*, the MDE1 nucleus-encoded factor required for *atpE* mRNA stabilization protects a specific 22-bp sequence in the 5′UTR of chloroplast-encoded *atpE* gene (Cavaiuolo et al., 2017, this work). Here, among a series of new ATP synthase mutants obtained, we have found that mutants *F28N* (*mde1-1*) and *E271* (*mde1-3*) carry insertions in the Cre08.g358530 gene, also mutated in *CAL014.01.30* (*mde1-2*). Using chloroplast transformation to replace the promoter and 5′-UTR of *atpE* with those of *psaA*, we demonstrated the genetic interaction between *MDE1* and *atpE*. MDE1, like many chloroplast-targeted RNA-binding factors (Hammani et al., 2014), contains OPR repeats, and we propose that it binds to the 22-bp target sequence to allow the stabilization of the *atpE* mono-cistron against 5′→3′ exonucleases, a scenario exemplified for *atpA* with MDA1 (Drapier et al., 2002; Viola et al., 2019), *atpB* with MDB1 (Jarrige, 2019), *atpH* with MTHI1 (Ozawa et al., 2020), *petA* with MCA1 (Boulouis et al., 2011; Loiselay et al., 2008), etc.

MDE1 has no orthologs in land plants, where no trans-acting factor is known for *aptE* which is co-transcribed downstream of *atpB*. In maize, the absence of the nucleus-encoded factors ATP1 and ATP4 impairs the translation of *atpB* but not the stability of *atpB*/*atpE* bicistronic mRNA nor the translation of *atpE* (Mc Cormac & Barkan, 1999; Zoschke et al., 2012, 2013). In tobacco, the *atpE* start codon is located within the *atpB* CDS but the bicistronic pre-mRNA is matured into distinct *atpB* and *atpE* mRNAs for translation (Kapoor et al., 1994). Notably, replacement of the Shine-Dalgarno (SD)-like sequence GGAG 15–18 bp upstream of the *atpE* initiation codon abolishes translation of *atpE* in tobacco (Hirose & Sugiura, 2004), but replacement of the SD-like sequence (GAAG) found 19–22 bp upstream of *atpE* start site in *C. reinhardtii* is not detrimental to translation (Fargo et al., 1998). Among green algae, the *atpE* gene, still found downstream of *atpB* in the early-diverging clades, in Ulvophyceae, and in basal Chlorophyceae such as *Neocystis brevis*, has relocated in most Chlorophyceae to downstream of *rps7* and acquired the conserved sequence that forms its 5′-end in *C. reinhardtii*. In some species, *atpE* can also be found downstream of *rps9*, *rpoC2*, *petG*, *trnC*, or *petA*, illustrating the high dynamics of chloroplast genome structure in Chlorophyceae. In many species, it probably carries its own promoter as in *C. reinhardtii*. Based on the presence of the *atpE* 5′ sequence and MDE1 orthologs in various algae, we propose that the former served as a stabilization element early after the gene was separated from *atpB*, but that its interaction with MDE1 occurred first in Chlamydomonadales. Has this interaction brought a selective advantage and how? In the diurnal cycle analysis (Strenkert et al., 2019), the MDE1 expression level peaks sharply half an hour after light is turned on, as is typical of genes involved in chloroplast gene expression. In other conditions, MDE1 levels could participate to a regulatory response, for instance, a downregulation of MDE1 levels upon nutrient deficiency shutting down the expression of *atpE*.

MATERIALS AND METHODS

Chlamydomonas reinhardtii strains, growth conditions, and genetic methods

Wild-type T222+ and mutant strains of *Chlamydomonas* were grown at 25°C in Tris-acetate-phosphate (TAP) medium, pH 7.2 or, when indicated, in minimal medium lacking acetate, pH 7.2 (Harris, 1989), under continuous low light (5 to 10 μmol photon m^{-2} sec^{-1}; white light-emitting diodes) unless otherwise specified. Crosses, tetrad dissection and random progeny analysis were performed according to Harris (1989). The deletion strains *ΔatpA*, *ΔatpH*, *ΔatpI*, as well as the chloroplast *atpF-Fud18* and *atpE-Fud17* mutants have been previously described (Drapier et al., 2007; Lemaire & Wollman, 1989b; Ozawa et al., 2020; Robertson et al., 1990). The nuclear *mdb1*, *mda1* and *mrl1* mutants impair *atpE*, *atpB* and *rbcL* mRNA accumulation, respectively (Drapier et al., 1992; Johnson et al., 2010; Viola et al., 2019), while the *atpC1* mutant lacks expression of the *ATPC* gene encoding the CF1 subunit γ (Smart & Selman, 1991, 1993). The nuclear mutant *ftsh1-1* expresses an inactive thylakoid FTSH protease (Malnoë et al., 2014). Except if specified otherwise, light levels are the following: low light: 5 μmol photon m^{-2} sec^{-1}, moderate light: 25 μmol photon m^{-2} sec^{-1}, high light: 200 μmol photon m^{-2} sec^{-1}.

Generation of ATP synthase mutants by random mutagenesis

The *F292*, *F28N*, *E236*, and *E271* mutants were generated in an effort to knock-out *FTSH2* and *EGY1* loci by CRISPR Cas9. We

© 2023 The Authors.

1365313x, 0, Downloaded from https://onlinelibrary.wiley.com/doi/10.1111/tpj.16448 by Portail BibCNRS INSB, Wiley Online Library on [28/11/2023]. See the Terms and Conditions (https://onlinelibrary.wiley.com/terms-and-conditions) on Wiley Online Library for rules of use; OA articles are governed by the applicable Creative Commons License

electroporated the DNA cassette containing the *aphVII* gene conferring resistance to antibiotic hygromycin in the presence of the Cas9 enzyme and RNA guides as described (Findinier et al., 2019). The RNA guides targeted sequences from *FTSH2* exon 3 (GCGAATCAGATCACGCTTGCCGG) or *EGY1* exon 1 (GTGCCAGCC TTTGGGTCATTGGG). Transformants were selected on TAP medium with hygromycin (20 mg L^{-1}) and screened for the light-sensitivity of photosynthetic electron transfer expected in *ftsh* or *egy1* mutants. However, the accumulation level of the thylakoid FTSH protease subunits FTSH1 and FTSH2, detected by immunoblot using anti-Var2 antibody (Figure S11), and PCR amplification of the *EGY1* targeted region in the *F292*, *F28N*, *E236* and *E271* mutants were similar to the WT strain, indicating that the *FTSH2* and *EGY1* loci were not affected. Back-crossing of these four ATP synthase mutants showed that the mutations were not genetically linked to hygromycin resistance. We reached the same conclusion for the non-photosynthetic mutant strain *CAL014.01.30* (*mde1-2*), obtained previously by insertional mutagenesis using the zeocin resistance gene *ble* (Dent et al., 2005).

Nucleic acid manipulations: DNA And constructs

Standard nucleic acid manipulations were performed according to Sambrook et al. (1989). The primers used in this study are listed in the Table S4. All DNA constructs were sequenced before transformation in *Chlamydomonas* and introduced by biolistic transformation (Boynton et al., 1988; Kuras & Wollman, 1994) for chloroplast transformation or by electroporation for nuclear transformation (see below).

Construction of the chimeric *5′psaA-atpE* gene

Plasmid P50 contains the 19.7 kbp Bam12 restriction fragment (Rochaix, 1978) cloned in the PUC8 vector, in an orientation that places the *psbA* gene close to the *Sma*I site of the multiple cloning site. To remove genes other than *atpE*, P50 was first digested by *Hpa*I and religated on itself to generate P50-H, which in turn was digested by *Sal*I and *Eco*RV, blunted with Klenow and religated on itself to yield p50-HSE. This latter plasmid was then digested with *Bam*HI and *Hpa*I, blunted with Klenow, and religated again on itself to create the p50Sh plasmid.

The chimeric 5′*psaA-atpE* gene was then generated by a two-step megaprime PCR procedure (Higuchi, 1990): primers psaA5U_F and psaAatpE_R were used to amplify a 262 bp fragment from template plasmid ps1A1 carrying *psaA* (Kück et al., 1987), while primers psaAatpE_F and atpE_PstI_R generated a 454 bp amplicon from template plasmid p50Sh. These two partially overlapping amplicons were mixed and used as templates in a third PCR reaction with the external primers psaA5U_F and atpE_PstI_R. The final amplicon (676 bp) was then digested with *Cla*I, blunted with Klenow and phenol-extracted, then digested with *Btg*I and cloned into the p50Sh vector digested by *Btg*I and *Bsa*BI to yield paAdE. The recycling 5′*psaA-aadA*$_{Exc}$ cassette, excised from plasmid p5′aA-aadA485 (Boulouis et al., 2015) by digestion with *Ale*I and *Xho*I, and blunted with Klenow, was cloned into plasmid paAdE, digested by *Avr*II and blunted with Klenow, in reverse orientation with respect to *atpE*, to yield plasmid pK^{r}aAdE that allows integration of the *aAdE* chimera at the *atpE* locus.

atpB deletion

Plasmid P-112, obtained from the *Chlamydomonas* Genetic Center (www.biology.duke.edu/chlamy/), contains a 5.3 kbp BamHI-EcoRI fragment from the chloroplast genome encompassing the *atpB* gene (Woessner et al., 1986), subcloned into pUC8 vector. The recycling 5′*psaA-aadA*$_{Exc}$ cassette, excised from plasmid p5′aA-aadA485 by digestion with *Ale*I and *Xho*I, and blunted with Klenow was cloned into plasmid P-112, digested with *Eco*RV and *Cla*I, itself blunted with Klenow, in direct orientation with respect to *atpB*.

Chlorophyll fluorescence analysis

We set a fast screening procedure by chlorophyll fluorescence imaging on plates with a time-resolved wide-angle camera (Johnson et al., 2009) to measure the ability to maintain PSII function upon short photo-inhibitory treatment. Using the method of weak detection pulses and saturating flash (Baker, 2008), we measured on each plate (i) the basal fluorescence F_0 and the maximal fluorescence F_M in the dark-adapted state, as well as (ii) transient fluorescence F′ and maximal fluorescence F_M' after 5 sec low light. The ratio F_V/F_M, where F_V=F_M-F_0, is the maximum PSII yield and depends almost exclusively on PSII function (e.g., PSII deficient mutants show F_V/F_M close to 0); in contrast, the PSII (operating) yield Y(II), defined as $(F_M'-F')/F_M'$, decreases when photosynthetic electron flow is limited (e.g., PSI deficient mutants show F_V/F_M similar to WT but Y(II) close to 0 even under low light).

Whole genome sequencing

We sequenced each strain by Illumina, using the NGSelect DNA data package (Eurofins, Germany), comprising the generation of a standard genomic library (DNA fragmentation, adapter ligation, size selection, and amplification) and data sequence of >5 million pair reads (2 × 151 bp). From these raw data, we identified mutations using the open-source platform Galaxy (usegalaxy.org) as follows. Paired-end reads raw data were treated with FASTQ groomer and their quality was confirmed using FASTQC. They were then mapped using the published workflow 'SNP calling on paired-end data' against the reference *C. reinhardtii* genome sequence computed for our WT strain T222+ by (Gallaher et al., 2015). Genomes were visualized using IGV (software.broadinstitute.org).

To map the *MDE1* locus, the *CAL014.01.30* mutant was back-crossed to the S1D2 strain, and the ATP synthase-deficient and wild-type progeny were separately pooled and sequenced. Reads were aligned onto the reference genome as above. Coverage of structural variants in the two pools of progeny was calculated across a 10 kb window (dots) and averaged with a sliding 100 kb window (curve) using Freebayes (Garrison & Marth, 2012), version 1.2.0, default except (--pooled-discrete --ploidy 2).

Protein isolation and immunoblot analysis

Thylakoid membranes were isolated as described (Chua & Bennoun, 1975). Before electrophoresis, proteins from whole cells or from thylakoid membranes were resuspended in 200 mM 1,4-DTT and 200 mM Na_2CO_3 and solubilized in the presence of 2% SDS at 100°C for 50 sec. Cell or thylakoid extracts were loaded on equal chlorophyll basis, separated by SDS-PAGE, and electro-transferred onto nitrocellulose membranes (Amersham Protran 0.1 μm NC) by semi-dry method. Membranes were stained in Ponceau for a loading control. Proteins were immunodetected by enhanced chemiluminescence. The blot membranes were incubated separately in primary antibodies against: AtpA (Drapier et al., 1992), AtpB (that recognizes CF1 β and F1 β; Atteia et al., 1992), ATPC (Agrisera AS08312), AtpE (Agrisera AS101590), ATPG (Agrisera AS09457), AtpH (Agrisera AS09591), cytochrome *f* and subunit IV of cytochrome b_6f (Kuras & Wollman, 1994), *Arabidopsis* FTSH2 named Var2 (Qi et al., 2016) that recognizes FTSH1 and FTSH2 in *Chlamydomonas* (Wang et al., 2017). Primary antibodies were revealed by horseradish peroxidase-conjugated antibodies against rabbit IgG

© 2023 The Authors.

1365313x, 0, Downloaded from https://onlinelibrary.wiley.com/doi/10.1111/tpj.16448 by Portail BibCNRS INSB, Wiley Online Library on [28/11/2023]. See the Terms and Conditions (https://onlinelibrary.wiley.com/terms-and-conditions) on Wiley Online Library for rules of use; OA articles are governed by the applicable Creative Commons License

(n° W401B, Promega). Heme *f* peroxidase activity was detected on blot membranes by chemiluminescence.

RNA isolation and analysis

Total RNAs were phenol-extracted, separated by electrophoresis on formaldehyde-agarose gels, transferred to membrane by capillarity and fixed at 80°C for 2 h in a vacuum-oven. RNA gel-blot analysis for Figure 5a were performed as described previously (Drapier et al., 2002) with ^{33}P-labeled probes derived from CDSs (Eberhard et al., 2002). For Northern blots of Figure S8, RNA were UV-crosslinked on the membrane and revealed with probes produced by PCR in the presence of digoxigenin-dUTP and thereby digoxigenin-labeled. After hybridization, the membrane was incubated in the presence of anti-digoxigenin antibody containing Fab fragment conjugated to alkaline phosphatase and revealed by chemiluminescence in the presence of CDP-Star reagent (Roche). Signals were acquired in a ChemiTouch imaging system (Bio-Rad). The probes for northern blot analyses were amplified using oligonucleotides indicated in Table S3.

CRISPR-Cas9 targeted gene knockouts

A custom protocol for generation of targeted gene knockouts was set up, based on multiple previous studies and aiming to promote insertion at the CRISPR-Cas9 cut site of a co-transformed Hygromycin resistance cassette (Berthold et al., 2002) as a selection marker, carrying homology flanks to promote insertion at the target locus *ATPG*. Guide RNAs were designed to cut within the first exon of the target gene, using CRISPOR-TEFOR predictor (http://crispor.tefor.net) based on the highest MIT Specificity score and the lowest off-target likelihood including mismatch (Concordet & Haeussler, 2018). Per reaction, 5 μg (30 pmol) recombinant Cas9, 0.25 μg *tracr* and 0.5 μg *cr* RNAs (all from Sigma Aldrich, respectively: CAS9PROT-250UG, TRACRRNAMOD-5NMOL and SygRNA (ATPG_288nt: 5′-AAGACCUGGUUCACCCCCGU, 5 nmol, modified)), giving a combined total of 0.75 μg *g*RNA, were mixed to reconstitute the RNP complex by incubation at 37°C for 30 min just before the transformation (similar to Dhokane et al., 2020; Findinier et al., 2019; Picariello et al., 2020; Shamoto et al., 2018). The Hygromycin resistance cassette was generated by PCR-amplification from plasmid *pSLHyg* by using dual-part primers (oZX119 and oZX120) containing on their 5′ side 40 nucleotides homologous to the *ATPG* regions flanking the predicted Cas9 cut site ('Hygro_HR' construct). As a control, the same cassette was PCR-amplified without homology arms ('Hygro' construct, primers: oZX_062 and oZX_063). In each case, 250 ng of PCR-purified product were used per transformation reaction. Because such a cassette generally integrates randomly in the genome, we tried to enhance homologous recombination by growing the cells under a light–dark cycle (Picariello et al., 2020) of 14 h at 100 μmol photons m^{-2} sec^{-1} at 25°C versus 10 h in darkness at 18°C (Greiner et al., 2017) in 100 ml TAP liquid culture to late exponential phase (≥4 10^6 cells ml^{-1}), timing the transformation to fall within a 1 h window prior to subjective dusk (Angstenberger et al., 2020). We used a cell-wall deficient strain (*cw15*) to increase efficiency (Picariello et al., 2020). ≥100 × 10^6 cells per transformation reaction (compared to 50 × 10^6 cells (Findinier et al., 2019; Picariello et al., 2020) and 500 × 10^6 cells (Dhokane et al., 2020)) were harvested by centrifugation (10 min, 1100 g, slow break) and resuspended in 250 μl TS40 (40 mM Sucrose in TAP), the transformation buffer used in many prior studies (Baek et al., 2016; Findinier et al., 2019; Kim et al., 2020; Park et al., 2020). To increase gene editing, cells were subjected to a 40°C heat shock for 30 min (Greiner et al., 2017; Park et al., 2020; Picariello et al., 2020). Cells, RNP and DNA were mixed in a 4 mm electroporation cuvette and incubated on ice (Angstenberger et al., 2020; Dhokane et al., 2020; Findinier et al., 2019; Shin et al., 2016) for 5 min. As a control, one batch of cells was transformed in the presence of the 'Hygro_HR' DNA but in absence of the RNP. To make sense of the widely varying electroporation parameters published previously, we calculated for each the estimated field strength by dividing Voltage by distance across the cuvette, and the estimated pulse duration by multiplying capacitance and resistance (μF × Ω = μs). An underlying consistency was revealed, with most authors using an estimated field strength between 1.5–2 kV cm^{-1} and a rough pulse duration estimate of 10–15 msec (Angstenberger et al., 2020; Ferenczi et al., 2017; Findinier et al., 2019; Kim et al., 2020; Picariello et al., 2020; Shamoto et al., 2018; Shin et al., 2016). A notable exception was the use of 2.5 kV cm^{-1} and 40 msec in (Dhokane et al., 2020), suggesting that walled cells may require stronger electroporation parameters. We thus chose to use 1.8 kV cm^{-1} and 15 msec which translates to 700 V, 50 μF and 300 Ω in our electroporation system (BioRad Gene Pulser II). Cells were subsequently transferred to 10 ml TS40 in 50 ml Falcon tubes and incubated in constant darkness (to avoid counter-selecting ATP-synthase mutants) over two nights (~42 h) in the diurnal incubator (to minimize stress).

ACKNOWLEDGEMENTS

We thank Marion Hamon and Christophe Marchand (IBPC, Paris) for the excellent proteomics analysis, Matthieu Mustas and Hugo Zalzalé for help respectively with chloroplast transformation and Northern analysis. We are grateful to Justin Findinier for his detailed protocol for CRISPR-Cas9 mediated mutagenesis, to Rachel Dent for the mutant strain *CAL014.01.30*, to Stephan Eberhard for insightful discussions, to Cheng Xie and Richard Jumar for explaining the physics of electroporators, and to Fei Yu for antibody against *Arabidopsis* FTSH2. This work was supported by the Centre national de la Recherche Scientifique and Sorbonne Université (basic support to Unité Mixte de Recherche 7141), by the 'Initiative d'Excellence' program from the French State (Grant 'DYNAMO', ANR-11-LABX-0011-01) and by the EQUIPEX CACSICE (ANR-11-EQPX-0008), notably through funding of the Proteomic Platform of IBPC (PPI). The PhD of Marcio Rodrigues-Azevedo was supported by a Ministry's doctoral contract and registered to the Doctoral School of Plant Sciences (SEVE) ED567, Université Paris-Saclay. Postdoctoral work by Oliver Caspari was supported by the ChloroMitoRAMP grant (ANR-19-CE13-0009).

AUTHOR CONTRIBUTIONS

FC and CV designed the research. FC, DJ, MR-A, S-IO, DD, OV, YC and CV performed the experiments. All authors analyzed the data. FC, ODC, OV, YC and CV wrote the original draft. All authors reviewed and edited the paper. CV coordinated the project.

SUPPORTING INFORMATION

Additional Supporting Information may be found in the online version of this article.

Figure S1. Sequencing reveals the insertion of transposon *TOC1* in the *ATPG* gene (Cre11.481450) of mutant *E236* and a single-nucleotide deletion in the *atpF* gene of mutant *Fud18*.

Figure S2. Genotyping of *F28N*, *CAL014.01.30* (I177), and *E271* identifies mutant alleles in the 1st exon of Cre08.g358530.t1.1.

© 2023 The Authors.

1365313x, 0, Downloaded from https://onlinelibrary.wiley.com/doi/10.1111/tpj.16448 by Portail BibCNRS INSB, Wiley Online Library on [28/11/2023]. See the Terms and Conditions (https://onlinelibrary.wiley.com/terms-and-conditions) on Wiley Online Library for rules of use; OA articles are governed by the applicable Creative Commons License

Figure S3. Distribution of proteins detected in less than two replicates in mutant *E236* and/or WT.

Figure S4. Restoration of ATP synthase membrane subunit AtpH accumulation in distinct *atpC1* and *ΔatpA* mutants by introgression of mutation in FTSH1 protease.

Figure S5. Analysis of CRISPR-Cas9-induced mutations of *ATPG* gene in NHEJ and HR clones.

Figure S6. Steps 2 and 3 in CRISPR-Cas9 workflow: second phenotyping and PCR genotyping of putative *atpG* mutants obtained by CRISPR-Cas9 edition.

Figure S7. Analysis of CRISPR-Cas9-induced mutations of *ATPG* gene in supplemental clones.

Figure S8. Northern blot analysis of chloroplast-encoded ATP synthase transcripts *atpA*, *atpB*, *atpH*, and *atpI*.

Figure S9. Restoration of ATP synthase in *mde1-2* and *mde1-3* mutant backgrounds by replacement of *atpE* 5′-UTR

Figure S10. Conservation of OPR domains in MDE1 orthologs.

Figure S11. Preliminary characterization of transformants.

Table S1. Sequencing datasets.

Table S2. Accession number for sequences used in Figure 6 and Figure S10.

Table S3. Oligonucleotides used to amplify the probes used for northern blot analyses.

Table S4. PCR primers list.

Table S5. Distribution of presence (orange background) or absence (grey background) of homology with the *C. reinhardtii* footprint within the 5′UTR *atpE*.

Table S6. Sites of homology with *C. reinhardtii* footprint within the 5′UTR *atpE*.

REFERENCES

Akiyama, Y., **Kihara, A.** & **Ito, K.** (1996) Subunit a of proton ATPase F0 sector is a substrate of the FtsH protease in *Escherichia coli*. *FEBS Letters*, **399**, 26–28. Available from: https://doi.org/10.1016/s0014-5793(96)01283-5

Angstenberger, M., **de Signori, F.**, **Vecchi, V.**, **Dall'Osto, L.** & **Bassi, R.** (2020) Cell synchronization enhances nuclear transformation and genome editing via Cas9 enabling homologous recombination in *Chlamydomonas reinhardtii*. *ACS Synthetic Biology*, **9**, 2840–2850. Available from: https://doi.org/10.1021/acssynbio.0c00390

Atteia, A., **de Vitry, C.**, **Pierre, Y.** & **Popot, J.L.** (1992) Identification of mitochondrial proteins in membrane preparations from *Chlamydomonas reinhardtii*. *The Journal of Biological Chemistry*, **267**, 226–234.

Baek, K., **Kim, D.H.**, **Jeong, J.**, **Sim, S.J.**, **Melis, A.**, **Kim, J.S.** ***et al.*** (2016) DNA-free two-gene knockout in *Chlamydomonas reinhardtii* via CRISPR-Cas9 ribonucleoproteins. *Scientific Reports*, **6**, 30620. Available from: https://doi.org/10.1038/srep30620

Bailleul, B., **Cardol, P.**, **Breyton, C.** & **Finazzi, G.** (2010) Electrochromism: a useful probe to study algal photosynthesis. *Photosynthesis Research*, **106**, 179–189. Available from: https://doi.org/10.1007/s11120-010-9579-z

Baker, N.R. (2008) Chlorophyll fluorescence: a probe of photosynthesis in vivo. *Annual Review of Plant Biology*, **59**, 89–113. Available from: https://doi.org/10.1146/annurev.arplant.59.032607.092759

Barkan, A., **Rojas, M.**, **Fujii, S.**, **Yap, A.**, **Chong, Y.S.**, **Bond, C.S.** ***et al.*** (2012) A combinatorial amino acid code for RNA recognition by pentatricopeptide repeat proteins. *PLoS Genetics*, **8**, e1002910. Available from: https://doi.org/10.1371/journal.pgen.1002910

Bennoun, P. & **Chua, N.H.** (1976) Methods for the detection and characterization of photosynthetic mutants in *Chlamydomonas reinhardtii*. In: Buchner, T. (Ed.) *Genetics and Biogenesis of Chloroplasts and Mitochondria*. Amsterdam: Elsevier/North-Holland Biomedical Press, pp. 33–39.

Bennoun, P., **Masson, A.** & **Delosme, M.** (1980) A method for complementation analysis of nuclear and chloroplast mutants of photosynthesis in *Chlamydomonas*. *Genetics*, **95**, 39–47. Available from: https://doi.org/10.1093/genetics/95.1.39

Berthold, P., **Schmitt, R.** & **Mages, W.** (2002) An engineered streptomyces hygroscopicus aph 7″ gene mediates dominant resistance against hygromycin B in *Chlamydomonas reinhardtii*. *Protist*, **153**, 401–412. Available from: https://doi.org/10.1078/14344610260450136

Boulouis, A., **Drapier, D.**, **Razafimanantsoa, H.**, **Wostrikoff, K.**, **Tourasse, N.J.**, **Pascal, K.** ***et al.*** (2015) Spontaneous dominant mutations in *Chlamydomonas* highlight ongoing evolution by gene diversification. *Plant Cell*, **27**, 984–1001. Available from: https://doi.org/10.1105/tpc.15.00010

Boulouis, A., **Raynaud, C.**, **Bujaldon, S.**, **Aznar, A.**, **Wollman, F.-A.** & **Choquet, Y.** (2011) The nucleus-encoded trans-acting factor MCA1 plays a critical role in the regulation of cytochrome f synthesis in *Chlamydomonas* chloroplasts. *Plant Cell*, **23**, 333–349. Available from: https://doi.org/10.1105/tpc.110.078170

Boynton, J.E., **Gillham, N.W.**, **Harris, E.H.**, **Hosler, J.P.**, **Johnson, A.M.**, **Jones, A.R.** ***et al.*** (1988) Chloroplast transformation in *Chlamydomonas* with high velocity microprojectiles. *Science*, **240**, 1534–1538. Available from: https://doi.org/10.1126/science.2897716

Bujaldon, S., **Kodama, N.**, **Rappaport, F.**, **Subramanyam, R.**, **de Vitry, C.**, **Takahashi, Y.** ***et al.*** (2017) Functional accumulation of antenna proteins in chlorophyll b-less mutants of *Chlamydomonas reinhardtii*. *Plant Molecular Biology*, **10**, 115–130. Available from: https://doi.org/10.1016/j.molp.2016.10.001

Calderon, R.H., **de Vitry, C.**, **Wollman, F.-A.** & **Niyogi, K.K.** (2023) Rubredoxin 1 promotes the proper folding of D1 and is not required for heme b_{559} assembly in *Chlamydomonas* photosystem II. *The Journal of Biological Chemistry*, **299**, 102968. Available from: https://doi.org/10.1016/j.jbc.2023.102968

Cavaiuolo, M., **Kuras, R.**, **Wollman, F.-A.**, **Choquet, Y.** & **Vallon, O.** (2017) Small RNA profiling in *Chlamydomonas*: insights into chloroplast RNA metabolism. *Nucleic Acids Research*, **45**, 10783–10799. Available from: https://doi.org/10.1093/nar/gkx668

Choquet, Y. & **Wollman, F.-A.** (2002) Translational regulations as specific traits of chloroplast gene expression. *FEBS Letters*, **529**, 39–42. Available from: https://doi.org/10.1016/s0014-5793(02)03260-x

Choquet, Y. & **Wollman, F.-A.** (2022) The assembly of photosynthetic proteins. In: Grossman, A.R. & Wollman, F.-A. (Eds.) *The Chlamydomonas sourcebook: Introduction to Chlamydomonas and its laboratory use. Organellar and Metabolic Processes*, Vol. **2**, 3rd edition. Amsterdam: Elsevier, pp. 615–646.

Chua, N.H. & **Bennoun, P.** (1975) Thylakoid membrane polypeptides of *Chlamydomonas reinhardtii*: wild-type and mutant strains deficient in photosystem II reaction center. *Proceedings of the National Academy of Sciences of the United States of America*, **72**, 2175–2179. Available from: https://doi.org/10.1073/pnas.72.6.2175

Cingolani, P., **Platts, A.**, **Wang le, L.**, **Coon, M.**, **Nguyen, T.**, **Wang, L.** ***et al.*** (2012) A program for annotating and predicting the effects of single nucleotide polymorphisms, SnpEff: SNPs in the genome of *Drosophila melanogaster* strain w1118; iso-2; iso-3. *Fly*, **6**, 80–92.

Concordet, J.-P. & **Haeussler, M.** (2018) CRISPOR: intuitive guide selection for CRISPR/Cas9 genome editing experiments and screens. *Nucleic Acids Research*, **46**, W242–W245. Available from: https://doi.org/10.1093/nar/gky354

Craig, R.J., **Hasan, A.R.**, **Ness, R.W.** & **Keightley, P.D.** (2021) Comparative genomics of *Chlamydomonas*. *Plant Cell*, **33**, 1016–1041.

Day, A. & **Rochaix, J.-D.** (1991) A transposon with an unusual LTR arrangement from *Chlamydomonas reinhardtii* contains an internal tandem array of 76 bp repeats. *Nucleic Acids Research*, **19**, 1259–1266. Available from: https://doi.org/10.1093/nar/19.6.1259

De Mia, M., **Lemaire, S.D.**, **Choquet, Y.** & **Wollman, F.-A.** (2019) Nitric oxide remodels the photosynthetic apparatus upon S-starvation in *Chlamydomonas reinhardtii*. *Plant Physiology*, **179**, 718–731. Available from: https://doi.org/10.1104/pp.18.01164

Del Cortona, A., **Jackson, C.J.**, **Bucchini, F.**, **Van Bel, M.**, **D'hondt, S.**, **Škaloud, P.** ***et al.*** (2020) Neoproterozoic origin and multiple transitions to macroscopic growth in green seaweeds. *Proceedings of the National Academy of Sciences of the United States of America*, **117**, 2551–2559. Available from: https://doi.org/10.1073/pnas.1910060117

Dent, R.M., **Haglund, C.M.**, **Chin, B.L.**, **Kobayashi, M.C.** & **Niyogi, K.K.** (2005) Functional genomics of eukaryotic photosynthesis using insertional mutagenesis of *Chlamydomonas reinhardtii*. *Plant Physiology*, **137**, 545–556. Available from: https://doi.org/10.1104/pp.104.055244

© 2023 The Authors.

1365313x, 0, Downloaded from https://onlinelibrary.wiley.com/doi/10.1111/tpj.16448 by Portail BibCNRS INSB, Wiley Online Library on [28/11/2023]. See the Terms and Conditions (https://onlinelibrary.wiley.com/terms-and-conditions) on Wiley Online Library for rules of use; OA articles are governed by the applicable Creative Commons License

Dhokane, D., **Bhadra, B.** & **Dasgupta, S.** (2020) CRISPR based targeted genome editing of *Chlamydomonas reinhardtii* using programmed Cas9-gRNA ribonucleoprotein. *Molecular Biology Reports*, **47**, 8747–8755. Available from: https://doi.org/10.1007/s11033-020-05922-5

Douglas, S.E. & **Penny, S.L.** (1999) The plastid genome of the cryptophyte alga, *Guillardia theta*: complete sequence and conserved syntheny groups confirm its common ancestry with red algae. *Journal of Molecular Evolution*, **48**, 238–244. Available from: https://doi.org/10.1007/pl00006462

Drager, R.G., **Girard-Bascou, J.**, **Choquet, Y.**, **Kindle, K.L.** & **Stern, D.B.** (1998) In vivo evidence for 5′→3′ exoribonuclease degradation of an unstable chloroplast mRNA. *The Plant Journal*, **13**, 85–96. Available from: https://doi.org/10.1046/j.1365-313x.1998.00016.x

Drapier, D., **Girard-Bascou, J.**, **Stern, D.B.** & **Wollman, F.-A.** (2002) A dominant nuclear mutation in *Chlamydomonas* identifies a factor controlling chloroplast mRNA stability by acting on the coding region of the atpA transcript. *The Plant Journal*, **31**, 687–697. Available from: https://doi.org/10.1046/j.1365-313x.2002.01387.x

Drapier, D., **Girard-Bascou, J.** & **Wollman, F.-A.** (1992) Evidence for nuclear control of the expression of the atpA and atpB chloroplast genes in *Chlamydomonas*. *Plant Cell*, **4**, 283–295. Available from: https://doi.org/10.1105/tpc.4.3.283

Drapier, D., **Rimbault, B.**, **Vallon, O.**, **Wollman, F.-A.** & **Choquet, Y.** (2007) Intertwined translational regulations set uneven stoichiometry of chloroplast ATP synthase subunits. *The EMBO Journal*, **26**, 3581–3591. Available from: https://doi.org/10.1038/sj.emboj.7601802

Eberhard, S., **Drapier, D.** & **Wollman, F.-A.** (2002) Searching limiting steps in the expression of chloroplast-encoded proteins: relations between gene copy number, transcription, transcript abundance and translation rate in the chloroplast of *Chlamydomonas reinhardtii*. *The Plant Journal*, **31**, 149–160. Available from: https://doi.org/10.1046/j.1365-313x.2002.01340.x

Eberhard, S., **Loiselay, C.**, **Drapier, D.**, **Bujaldon, S.**, **Girard-Bascou, J.**, **Kuras, R.** ***et al.*** (2011) Dual functions of the nucleus-encoded factor TDA1 in trapping and translation activation of atpA transcripts in *Chlamydomonas reinhardtii* chloroplasts. *The Plant Journal*, **67**, 1055–1066. Available from: https://doi.org/10.1111/j.1365-313X.2011.04657.x

Fargo, D.C., **Zhang, M.**, **Gillham, N.W.** & **Boynton, J.E.** (1998) Shine-Dalgarno-like sequences are not required for translation of chloroplast mRNAs in *Chlamydomonas reinhardtii* chloroplasts or in *Escherichia coli*. *Molecular & General Genetics*, **257**, 271–282. Available from: https://doi.org/10.1007/s004380050648

Ferenczi, A., **Pyott, D.E.**, **Xipnitou, A.** & **Molnar, A.** (2017) Efficient targeted DNA editing and replacement in *Chlamydomonas reinhardtii* using Cpf1 ribonucleoproteins and single-stranded DNA. *Proceedings of the National Academy of Sciences of the United States of America*, **114**, 13567–13572. Available from: https://doi.org/10.1073/pnas.1710597114

Finazzi, G., **Drapier, D.** & **Rappaport, F.** (2009) The CF_0F_1 ATP synthase complex of photosynthesis. In: Stern, D. (Ed.) *The Chlamydomonas Sourcebook Second Edition. Organella and Metabolic Processes*, Vol. **2**. Amsterdam: Elsevier, Academic Press, pp. 639–670 ISBN 0080919561, 9780080919560.

Findinier, J., **Delevoye, C.** & **Cohen, M.M.** (2019) The dynamin-like protein Fzl promotes thylakoid fusion and resistance to light stress in *Chlamydomonas reinhardtii*. *PLoS Genetics*, **15**, e1008047. Available from: https://doi.org/10.1371/journal.pgen.1008047

Gallaher, S.D., **Fitz-Gibbon, S.T.**, **Glaesener, A.G.**, **Pellegrini, M.** & **Merchant, S.S.** (2015) *Chlamydomonas* genome resource for laboratory strains reveals a mosaic of sequence variation, identifies true strain histories, and enables strain-specific studies. *Plant Cell*, **27**, 2335–2352. Available from: https://doi.org/10.1105/tpc.15.00508

Gallaher, S.D., **Fitz-Gibbon, S.T.**, **Strenkert, D.**, **Purvine, S.O.**, **Pellegrini, M.** & **Merchant, S.S.** (2018) High-throughput sequencing of the chloroplast and mitochondrion of *Chlamydomonas reinhardtii* to generate improved de novo assemblies, analyze expression patterns and transcript speciation, and evaluate diversity among laboratory strains and wild isolates. *The Plant Journal*, **93**, 545–565. Available from: https://doi.org/10.1111/tpj.13788

Garrison, E. & **Marth, G.** (2012) Haplotype-based variant detection from short-read sequencing. *arXiv*, 1207.3907. Available from: https://doi.org/10.48550/arXiv.1207.3907

Greiner, A., **Kelterborn, S.**, **Evers, H.**, **Kreimer, G.**, **Sizova, I.** & **Hegemann, P.** (2017) Targeting of photoreceptor genes in *Chlamydomonas reinhardtii* via zinc-finger nucleases and CRISPR/Cas9. *Plant Cell*, **29**, 2498–2518. Available from: https://doi.org/10.1105/tpc.17.00659

Guélin, E., **Rep, M.** & **Grivell, L.A.** (1996) Afg3p, a mitochondrial ATP-dependent metalloprotease, is involved in the degradation of mitochondrially encoded Cox1, Cox3, cob, Su6, Su8 and Su9 subunits of the inner membrane complexes III, IV and V. *FEBS Letters*, **381**, 42–46. Available from: https://doi.org/10.1016/0014-5793(96)00074-9

Hahn, A., **Vonck, J.**, **Mills, D.J.**, **Meier, T.** & **Kühlbrandt, W.** (2018) Structure, mechanism, and regulation of the chloroplast ATP synthase. *Science*, **360**, eaat4318. Available from: https://doi.org/10.1126/science.aat4318

Hammani, K., **Bonnard, G.**, **Bouchoucha, A.**, **Gobert, A.**, **Pinker, F.**, **Salinas, T.** ***et al.*** (2014) Helical repeats modular proteins are major players for organelle gene expression. *Biochimie*, **100**, 141–150. Available from: https://doi.org/10.1016/j.biochi.2013.08.031

Harris, E.H. (1989) *The Chlamydomonas Sourcebook: A comprehensive guide to biology and laboratory use*. San Diego: Elsevier, Academic Press.

Higuchi, R. (1990) Recombinant PCR. In *PCR protocols: A guide to methods and application*. London, New York: Academic Press.

Hirose, T. & **Sugiura, M.** (2004) Functional Shine-Dalgarno-like sequences for translational initiation of chloroplast mRNAs. *Plant & Cell Physiology*, **45**, 114–117. Available from: https://doi.org/10.1093/pcp/pch002

Jarrige, D. (2019) *Deciphering the "OPR code" to further assess the physiological roles of OPR proteins*. PhD Thesis. Paris: Sorbonne Université.

Johnson, X. (2011) Manipulating RuBisCO accumulation in the green alga, *Chlamydomonas reinhardtii*. *Plant Molecular Biology*, **76**, 397–405. Available from: https://doi.org/10.1007/s11103-011-9783-z

Johnson, X., **Vandystadt, G.**, **Bujaldon, S.**, **Wollman, F.A.**, **Dubois, R.**, **Roussel, P.** ***et al.*** (2009) A new setup for in vivo fluorescence imaging of photosynthetic activity. *Photosynthesis Research*, **102**, 85–93. Available from: https://doi.org/10.1007/s11120-009-9487-2

Johnson, X., **Wostrikoff, K.**, **Finazzi, G.**, **Kuras, R.**, **Schwarz, C.**, **Bujaldon, S.** ***et al.*** (2010) MRL1, a conserved pentatricopeptide repeat protein, is required for stabilization of rbcL mRNA in *Chlamydomonas* and *Arabidopsis*. *Plant Cell*, **22**, 234–248. Available from: https://doi.org/10.1105/tpc.109.066266

Kapoor, S., **Wakasugi, T.**, **Deno, H.** & **Sugiura, M.** (1994) An atpE-specific promoter within the coding region of the atpB gene in tobacco chloroplast DNA. *Current Genetics*, **26**, 263–268. Available from: https://doi.org/10.1007/BF00309558

Kato, Y., **Kuroda, H.**, **Ozawa, S.-I.**, **Saito, K.**, **Dogra, V.**, **Scholz, M.** ***et al.*** (2023) Characterization of tryptophan oxidation affecting D1 degradation by FtsH in the photosystem II quality control of chloroplasts. *eLife*, **12**, RP88822. Available from: https://doi.org/10.7554/eLife.88822.1

Ketchner, S.L., **Drapier, D.**, **Olive, J.**, **Gaudriault, S.**, **Girard-Bascou, J.** & **Wollman, F.-A.** (1995) Chloroplasts can accommodate inclusion bodies: evidence from a mutant of *Chlamydomonas reinhardtii* defective in the assembly of the chloroplast ATP synthase. *The Journal of Biological Chemistry*, **270**, 15299–152306. Available from: https://doi.org/10.1074/jbc.270.25.15299

Kim, J., **Lee, S.**, **Baek, K.** & **Jin, E.S.** (2020) Site-specific gene knock-out and on-site heterologous gene overexpression in *Chlamydomonas reinhardtii* via a CRISPR-Cas9-mediated knock-in method. *Frontiers in Plant Science*, **11**, 306. Available from: https://doi.org/10.3389/fpls.2020.00306

Kim, K.S., **Kustu, S.** & **Inwood, W.** (2006) Natural history of transposition in the green alga *Chlamydomonas reinhardtii*: use of the AMT4 locus as an experimental system. *Genetics*, **173**, 2005–2019. Available from: https://doi.org/10.1534/genetics.106.058263

Kong, M.M., **Wang, F.F.**, **Yang, Z.N.** & **Mi, H.L.** (2013) ATPG is required for the accumulation of chloroplast ATP synthase in Arabidopsis. *Chinese Science Bulletin*, **58**, 3224–3232. Available from: https://doi.org/10.1007/s11434-013-5916-x

Kück, U., **Choquet, Y.**, **Schneider, M.**, **Dron, M.** & **Bennoun, P.** (1987) Structural and transcription analysis of two homologous genes for the P700 chlorophyll a-apoproteins in *Chlamydomonas*: evidence for in vivo transsplicing. *The EMBO Journal*, **6**, 2185–2195. Available from: https://doi.org/10.1002/j.1460-2075.1987.tb02489.x

Kuras, R. & **Wollman, F.-A.** (1994) The assembly of cytochrome b6/f complexes: An approach using genetic transformation of the green alga

© 2023 The Authors.

1365313x, 0, Downloaded from https://onlinelibrary.wiley.com/doi/10.1111/tpj.16448 by Portail BibCNRS INSB, Wiley Online Library on [28/11/2023]. See the Terms and Conditions (https://onlinelibrary.wiley.com/terms-and-conditions) on Wiley Online Library for rules of use; OA articles are governed by the applicable Creative Commons License

Chlamydomonas reinhardtii. *The EMBO Journal*, **13**, 1019–1027. Available from: https://doi.org/10.1002/j.1460-2075.1994.tb06350.x

Lemaire, C. & **Wollman, F.-A.** (1989a) The chloroplast ATP synthase in *Chlamydomonas reinhardtii*. I. Characterization of its nine constitutive subunits. *The Journal of Biological Chemistry*, **264**, 10228–10234 PMID: 2524491.

Lemaire, C. & **Wollman, F.-A.** (1989b) The chloroplast ATP synthase in *Chlamydomonas reinhardtii*. II. Biochemical studies on its biogenesis using mutants defective in photophosphorylation. *The Journal of Biological Chemistry*, **264**, 10235–10242 PMID: 2524492.

Lemaire, C., **Wollman, F.-A.** & **Bennoun, P.** (1988) Restoration of phototrophic growth in a mutant of *Chlamydomonas reinhardtii* in which the chloroplast atpB gene of the ATP synthase has a deletion: an example of mitochondria-dependent photosynthesis. *Proceedings of the National Academy of Sciences of the United States of America*, **85**, 1344–1348. Available from: https://doi.org/10.1073/pnas.85.5.1344

Loiselay, C., **Gumpel, N.J.**, **Girard-Bascou, J.**, **Watson, A.T.**, **Purton, S.**, **Wollman, F.-A.** ***et al.*** (2008) Molecular identification and function of cis- and trans-acting determinants for petA transcript stability in *Chlamydomonas reinhardtii* chloroplasts. *Molecular and Cellular Biology*, **28**, 5529–5542. Available from: https://doi.org/10.1128/MCB.02056-07

Majeran, W., **Olive, J.**, **Drapier, D.**, **Vallon, O.** & **Wollman, F.-A.** (2001) The light sensitivity of ATP synthase mutants of *Chlamydomonas reinhardtii*. *Plant Physiology*, **126**, 421–433. Available from: https://doi.org/10.1104/pp.126.1.421

Majeran, W., **Wostrikoff, K.**, **Wollman, F.-A.** & **Vallon, O.** (2019) Role of ClpP in the biogenesis and degradation of RuBisCO and ATP synthase in *Chlamydomonas reinhardtii*. *Plants*, **8**, 191. Available from: https://doi.org/10.3390/plants8070191

Malik Ghulam, M., **Zghidi-Abouzid, O.**, **Lambert, E.**, **Lerbs-Mache, S.** & **Merendino, L.** (2012) Transcriptional organization of the large and the small ATP synthase operons, atpI/H/F/a and atpB/E, in Arabidopsis thaliana chloroplasts. *Plant Molecular Biology*, **79**, 259–272. Available from: https://doi.org/10.1007/s11103-012-9910-5

Malnoë, A., **Wang, F.**, **Girard-Bascou, J.**, **Wollman, F.A.** & **de Vitry, C.** (2014) Thylakoid FtsH protease contributes to photosystem II and cytochrome b6f remodeling in *Chlamydomonas reinhardtii* under stress conditions. *Plant Cell*, **26**, 373–390. Available from: https://doi.org/10.1105/tpc.113.120121

Malnoë, A., **Wollman, F.A.**, **de Vitry, C.** & **Rappaport, F.** (2011) Photosynthetic growth despite a broken Q-cycle. *Nature Communications*, **2**, 301. Available from: https://doi.org/10.1038/ncomms1299

Mc Cormac, D.J. & **Barkan, A.** (1999) A nuclear gene in maize required for the translation of the chloroplast atpB/E mRNA. *Plant Cell*, **11**, 1709–1716. Available from: https://doi.org/10.1105/tpc.11.9.1709

Merchant, S.S., **Prochnik, S.E.**, **Vallon, O.**, **Harris, E.H.**, **Karpowicz, S.J.**, **Witman, G.B.** ***et al.*** (2007) The *Chlamydomonas* genome reveals the evolution of key animal and plant functions. *Science*, **318**, 245–250. Available from: https://doi.org/10.1126/science.1143609

O'Donnell, S., **Chaux, F.** & **Fischer, G.** (2020) Highly contiguous nanopore genome assembly of *Chlamydomonas reinhardtii* CC-1690. *Microbiology Resource Announcements*, **9**, e00726. Available from: https://doi.org/10.1128/MRA.00726-20

Oudot-le Secq, M.-P., **Grimwood, J.**, **Shapiro, H.**, **Armbrust, E.V.**, **Bowler, C.** & **Green, B.R.** (2007) Chloroplast genomes of the diatoms *Phaeodactylum tricornutum* and *Thaliassiosira pseudonana*: comparison with other plastid genomes of the red lineage. *Molecular Genetics and Genomics*, **277**, 427–439. Available from: https://doi.org/10.1007/s00438-006-0199-4

Ozawa, S.-I., **Cavaiuolo, M.**, **Jarrige, D.**, **Kuras, R.**, **Rutgers, M.**, **Eberhard, S.** ***et al.*** (2020) The OPR protein MTHI1 controls the expression of two different subunits of ATP synthase CFo in *Chlamydomonas reinhardtii*. *Plant Cell*, **32**, 1179–1203. Available from: https://doi.org/10.1105/tpc.19.00770

Pajic, A., **Tauer, R.**, **Feldmann, H.**, **Neupert, W.** & **Langer, T.** (1994) Yta10p is required for the ATP-dependent degradation of polypeptides in the inner membrane of mitochondria. *FEBS Letters*, **353**, 201–206. Available from: https://doi.org/10.1016/0014-5793(94)01046-3

Park, R.V., **Asbury, H.** & **Miller, S.M.** (2020) Modification of a *Chlamydomonas reinhardtii* CRISPR/Cas9 transformation protocol for use with widely available electroporation equipment. *MethodsX*, **7**, 100855. Available from: https://doi.org/10.1016/j.mex.2020.100855

Pfalz, J., **Bayraktar, O.A.**, **Prikryl, J.** & **Barkan, A.** (2009) Site-specific binding of a PPR protein defines and stabilizes 5′ and 3′ mRNA termini in chloroplasts. *The EMBO Journal*, **28**, 2042–2052. Available from: https://doi.org/10.1038/emboj.2009.12

Picariello, T., **Hou, Y.**, **Kubo, T.**, **McNeill, N.A.**, **Yanagisawa, H.-A.**, **Oda, T.** ***et al.*** (2020) TIM, a targeted insertional mutagenesis method utilizing CRISPR/Cas9 in *Chlamydomonas reinhardtii*. *PLoS One*, **15**, e0232594. Available from: https://doi.org/10.1371/journal.pone.0232594

Qi, Y., **Liu, X.**, **Liang, S.**, **Wang, R.**, **Li, Y.**, **Zhao, J.** ***et al.*** (2016) A putative chloroplast thylakoid metalloprotease VIRESCENT3 regulates chloroplast development in *Arabidopsis thaliana*. *The Journal of Biological Chemistry*, **291**, 3319–3332. Available from: https://doi.org/10.1074/jbc.M115.681601

Robertson, D., **Boynton, J.E.** & **Gillham, N.W.** (1990) Cotranscription of the wild-type chloroplast atpE gene encoding CF1/CF0 epsilon subunit with the 3′ half of the rps7 gene in *Chlamydomonas reinhardtii* and characterization of frameshift mutations in atpE. *Molecular & General Genetics*, **221**, 155–163. Available from: https://doi.org/10.1007/BF00261715

Rochaix, J.-D. (1978) Restriction endonuclease map of the chloroplast DNA of *Chlamydomonas reinhardtii*. *Journal of Molecular Biology*, **126**, 597–617. Available from: https://doi.org/10.1016/0022-2836(78)90011-6

Rühle, T. & **Leister, D.** (2015) Assembly of F1F0-ATP synthases. *Biochimica et Biophysica Acta*, **1847**, 849–860. Available from: https://doi.org/10.1016/j.bbabio.2015.02.005

Sambrook, J., **Fritsch, E.F.** & **Maniatis, T.** (1989) *Molecular cloning*. Cold Spring Harbor: Cold Spring harbor Laboratory Press.

Schroda, M., and **de Vitry, C.** (2022) Molecular chaperones, proteases, and unfolded protein responses. In *The* Chlamydomonas *sourcebook: Introduction to* Chlamydomonas *and its laboratory use (Grossman, A. R. and Wollman, F.-A., eds.),* Organellar and Metabolic Processes, vol. *2. Elsevier, Amsterdam, 3rd edition, pp. 647–689.*

Shamoto, N., **Narita, K.**, **Kubo, T.**, **Oda, T.** & **Takeda, S.** (2018) CFAP70 is a novel axoneme-binding protein that localizes at the base of the outer dynein arm and regulates ciliary motility. *Cell*, **7**, 124. Available from: https://doi.org/10.3390/cells7090124

Shin, S.E., **Lim, J.M.**, **Koh, H.G.**, **Kim, E.K.**, Kang, N.K **Kang N.K.**, **Jeon S.**, **Kwon S.**, **Shin W.S.**, **Lee B.**, **Hwangbo K.**, **Kim J.**, **Ye S.H.**, **Yun J.Y.**, **Seo H.**, **Oh H.M.**, **Kim K.J.**, **Kim J.S.**, **Jeong W.J.**, **Chang Y.K.**, **Jeong B.R.** (2016) CRISPR/Cas9-induced knockout and knockin mutations in *Chlamydomonas reinhardtii*. *Scientific Reports*, **6**, 27810. https://doi.org/10.1038/srep27810

Smart, E.J. & **Selman, B.R.** (1991) Isolation and characterization of a *Chlamydomonas reinhardtii* mutant lacking the gamma-subunit of chloroplast coupling factor 1 (CF1). *Molecular and Cellular Biology*, **11**, 5053–5058. Available from: https://doi.org/10.1128/mcb.11.10.5053-5058.1991

Smart, E.J. & **Selman, B.R.** (1993) Complementation of a *Chlamydomonas reinhardtii* mutant defective in the nuclear gene encoding the chloroplast coupling factor 1 (CF1) gamma-subunit (atpC). *Journal of Bioenergetics and Biomembranes*, **25**, 275–284. Available from: https://doi.org/10.1007/BF00762588

Strenkert, D., **Schmollinger, S.**, **Gallaher, S.D.**, **Salomé, P.A.**, **Purvine, S.O.**, **Nicora, C.D.** ***et al.*** (2019) Multiomics resolution of molecular events during a day in the life of *Chlamydomonas*. *Proceedings of the National Academy of Sciences of the United States of America*, **116**, 2374–2383. Available from: https://doi.org/10.1073/pnas.1815238116

Tourasse, N., **Choquet, Y.** & **Vallon, O.** (2013) PPR proteins of green algae. *RNA Biology*, **10**, 1526–1542. Available from: https://doi.org/10.4161/rna.26127

Vaistij, F.E., **Boudreau, E.**, **Lemaire, S.D.**, **Goldschmidt-Clermont, M.** & **Rochaix, J.-D.** (2000) Characterization of Mbb1, a nucleus-encoded tetratricopeptide-like repeat protein required for expression of the chloroplast psbB/psbT/psbH gene cluster in *Chlamydomonas reinhardtii*. *Proceedings of the National Academy of Sciences of the United States of America*, **97**, 14813–14818. Available from: https://doi.org/10.1073/pnas.97.26.14813

van Wijk, K.J. (2015) Protein maturation and proteolysis in plant plastids, mitochondria and peroxisomes. *Annual Review of Plant Biology*, **66**, 75–111. Available from: https://doi.org/10.1146/annurev-arplant-043014-115547

Viola, S., **Cavaiuolo, M.**, **Drapier, D.**, **Eberhard, S.**, **Vallon, O.**, **Wollman, F.-A.** ***et al.*** (2019) MDA1, a nucleus encoded factor involved in the stabilization and processing of the atpA transcript in the chloroplast of

© 2023 The Authors.

1365313x, 0, Downloaded from https://onlinelibrary.wiley.com/doi/10.1111/tpj.16448 by Portail BibCNRS INSB, Wiley Online Library on [28/11/2023]. See the Terms and Conditions (https://onlinelibrary.wiley.com/terms-and-conditions) on Wiley Online Library for rules of use; OA articles are governed by the applicable Creative Commons License

Chlamydomonas. *The Plant Journal*, **98**, 1033–1047. Available from: https://doi.org/10.1111/tpj.14300

Wang, F., **Johnson, X.**, **Cavaiuolo, M.**, **Bohne, A.V.**, **Nickelsen, J.** & **Vallon, O.** (2015) Two *Chlamydomonas* OPR proteins stabilize chloroplast mRNAs encoding small subunits of photosystem II and cytochrome b6 f. *The Plant Journal*, **82**, 861–873. Available from: https://doi.org/10.1111/tpj.12858

Wang, F., **Qi, Y.**, **Malnoë, A.**, **Choquet, Y.**, **Wollman, F.-A.** & **de Vitry, C.** (2017) The high light response and redox control of thylakoid protease in *Chlamydomonas reinhardtii*. *Molecular Plant*, **10**, 99–114. Available from: https://doi.org/10.1016/j.molp.2016.09.012

Wei, L., **Derrien, B.**, **Gautier, A.**, **Houilles-Vernes, L.**, **Boulouis, A.**, **Saint-Marcoux, D.** ***et al.*** (2014) Nitric oxide-triggered remodeling of chloroplast bioenergetics and thylakoid proteins upon nitrogen starvation in *Chlamydomonas reinhardtii*. *Plant Cell*, **26**, 353–372. Available from: https://doi.org/10.1105/tpc.113.120121

Woessner, J.P., **Gillham, N.W.** & **Boynton, J.E.** (1986) The sequence of the chloroplast atpB gene and its flanking regions in *Chlamydomonas reinhardtii*. *Gene*, **44**, 17–28. Available from: https://doi.org/10.1016/0378-1119(86)90038-7

Yan, J., **Yao, Y.**, **Hong, S.**, **Yang, Y.**, **Shen, C.**, **Zhang, Q.** ***et al.*** (2019) Delineation of pentatricopeptide repeat codes for target RNA prediction. *Nucleic Acids Research*, **47**, 3728–3738. Available from: https://doi.org/10.1093/nar/gkz075

Zoschke, R., **Kroeger, T.**, **Belcher, S.**, **Schöttler, M.A.**, **Barkan, A.** & **Schmitz-Linneweber, C.** (2012) The pentatricopeptide repeat-SMR protein ATP4 promotes translation of the chloroplast atpB/E mRNA. *The Plant Journal*, **72**, 547–558. Available from: https://doi.org/10.1111/j.1365-313X.2012.05081.x

Zoschke, R., **Watkins, K.P.** & **Barkan, A.** (2013) A rapid ribosome profiling method elucidates chloroplast ribosome behavior in vivo. *Plant Cell*, **25**, 2265–2275. Available from: https://doi.org/10.1105/tpc.113.111567

© 2023 The Authors.

1365313x, 0, Downloaded from https://onlinelibrary.wiley.com/doi/10.1111/tpj.16448 by Portail BibCNRS INSB, Wiley Online Library on [28/11/2023]. See the Terms and Conditions (https://onlinelibrary.wiley.com/terms-and-conditions) on Wiley Online Library for rules of use; OA articles are governed by the applicable Creative Commons License